GROUNDWATER MODEL STUDYING EFFECTS OF EXISTING RECHARGE BASIN AND PROPOSED SUBSURFACE BARRIER FOR A RANCH IN SANTA ROSA CREEK WATERSHED

A Thesis

presented to

the Faculty of California Polytechnic State University,

San Luis Obispo

In Partial Fulfillment

of the Requirements for the Degree

Master of Science in Civil and Environmental Engineering

by

Stefan Jetton Young

June 2021

COMMITTEE MEMBERSHIP

TITLE:	Groundwater Model Studying Effects of Existing Recharge Basin and Proposed Subsurface Barrier for a Ranch in Santa Rosa Creek Watershed
AUTHOR:	Stefan Jetton Young
DATE SUBMITTED:	June 2021
COMMITTEE CHAIR:	Misgana Muleta, Ph.D., PE., D.WRE Professor of Civil and Environmental Engineering
COMMITTEE MEMBER:	Derek Manheim, Ph.D., Lecturer and Research Fellow
COMMITTEE MEMBER:	Aleksandra Wydzga, PH, Senior Hydrologist at Creek Lands Conservation and Adjunct Faculty at California Polytechnic State University, San Luis Obispo

ABSTRACT

Groundwater Model Studying Effects of Existing Recharge Basin and Proposed Subsurface Barrier for a Ranch in Santa Rosa Creek Watershed

Stefan Jetton Young

A groundwater model of a 126.2-acre ranch in Cambria, California was expanded upon to analyze the effects of artificial recharge and a subsurface barrier. The ranch lies within the $48mi^2$ Santa Rosa Creek Watershed along the Central Coast of California. The mainly agricultural watershed outfalls to the Pacific Ocean to its west. Creek Lands Conservation, a non-profit that aims to conserve and restore habitat along the Central Coast, plans to identify projects to restore stream flow during dry seasons in the creek that runs through the Santa Rosa Creek Watershed and to increase artificial groundwater recharge. This study focuses on two of those projects. One project is an existing recharge basin and the other is a subsurface barrier. The objective of this numerical model is to improve upon an existing model by using a longer duration of data to calibrate the model, calibrating the model to hydraulic properties of soil samples that were obtained from the site at various depths, refining elevations of layers through integration of new borehole exploration data, and adding updated and new data such as mountain front recharge and pumping rates. The modeling program used was GMS which allows calculation and determination of heads and flow directions. Within the model, there are three separate layers based on hydrogeological characterization from previous studies. There is an upper unconfined zone, a confining clay layer, and a confined zone. A package within GMS (Groundwater Modeling System) called PEST (i.e., Parameter ESTimation) was used to calibrate the model to known water surface elevations throughout the site. Data such as elevations, head boundaries, stream flow, pumping rates, recharge, evapotranspiration, well locations, and hydraulic properties of the subsurface was processed and incorporated into the overall model in GMS. Recharge rates from the basin were estimated to be 0.1 m/day roughly starting in February and ending in May for each year. The model showed that the confining layer slows down the flow of water from the recharge basin, but it does eventually percolate into the underlying groundwater aquifer before reaching Santa Rosa Creek after a time period of 5 years. The proposed subsurface barrier does reduce travel times of groundwater by roughly a year and helps percolation of water into the confined layer. With the subsurface barrier it was seen that the water held within the confined aquifer increased on average 5,200 m^3 each year.

ACKNOWLEDGMENTS

I am beyond grateful to those that have helped me in my finishing my thesis during this COVID-19 pandemic and the limitations it has placed on our communities. I first want to thank my advisor, Dr. Muleta, for your time and guidance with helping me with the completion of this thesis. The commitment that you have taken on with helping with my senior project through this thesis all while helping out many other students at the same time is inspiring.

I would like to thank my committee member, Dr. Manheim, who taught me the modeling program and was always there to answer questions regarding the program. I am also thankful for the other committee member, Aleksandra Wyzdga, for her non-profit and all the background information for the thesis. Thank you to Nephi Derbidge for helping me get access to Cal Poly's Geotechnical Engineering Lab and teaching me how to run tests on soil samples for my thesis research. I would also like to thank Alex Murray who started research on this topic and provided a great foundation for me to help expand on the modeling and research for this thesis.

Lastly, I want to thank everyone who has supported me along my college experience from my coaches and teammates on the Cal Poly Swim and Dive team to my friends, who all encouraged me. I also am truly thankful for my family who supported me every step of the way.

TABLE OF CONTENTS

LIST OF TABLES

LIST OF FIGURES

CHAPTER 1. INTRODUCTION

Groundwater is a heavily relied upon source of water stored in geological formations, called aquifers, that are made up of soil and fractured rock beneath the surface of the Earth. Water moves through soil and rock at speeds that are dependent on the size of the pores and how well the pores are interconnected in the non-saturated zone, and within the saturated zone pressure differences drive the flow of water. Water tables can be deep or shallow, while also rising or falling depending on factors that can include precipitation and extraction. Approximately 30 to 40% of California's total water supply originates from groundwater in normal to wet years and up to 58% during dry years (DWR, 2021) (Figure 1). Figure 1 shows the annual groundwater use as a part of the total water use in California from 2002-2016. For most rural areas in California, 100% of the water supply is sourced from groundwater.

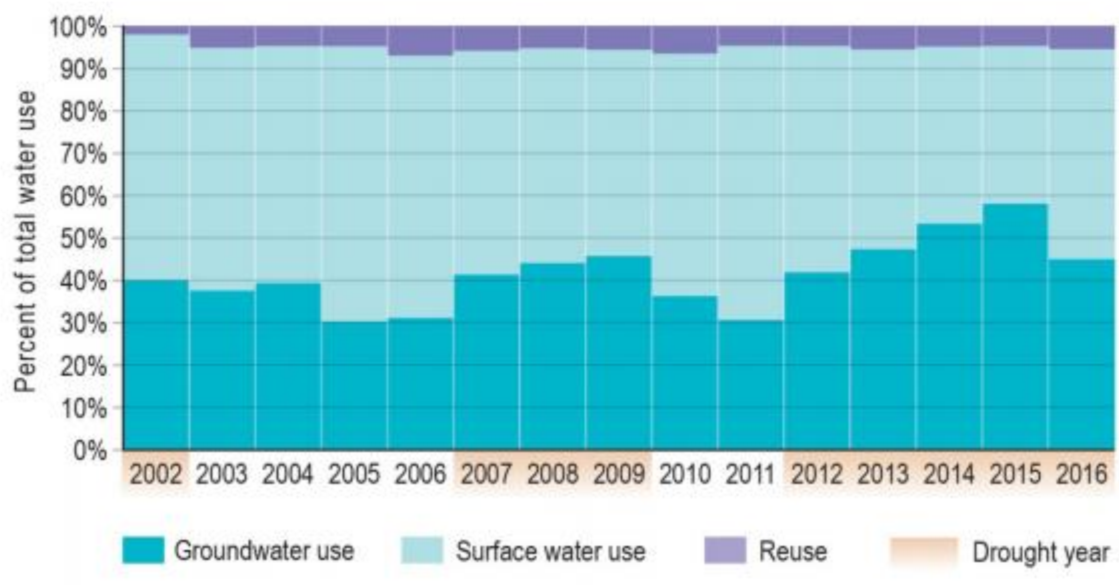

Figure 1: Annual Water Use in California from 2002-2016 (DWR, 2021)

Groundwater is accessed mostly through wells and pumps. Figure 2 illustrates the amount of groundwater used for agricultural and urban purposes from 2002 to 2016. It can be seen that agriculture dominates the total usage, especially during drought periods.

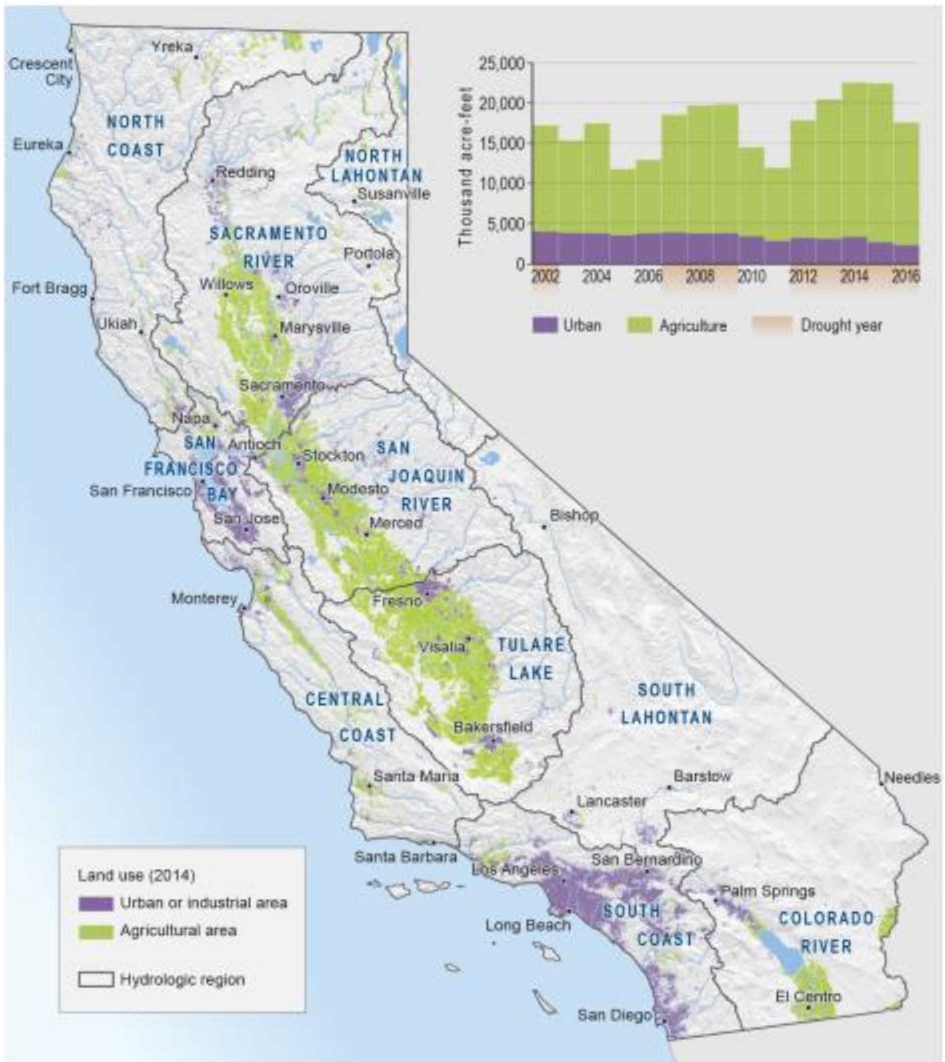

Figure 2: Groundwater use in Agricultural and Urban Areas from 2002-2016 (DWR, 2021)

Over the past decade, California has experienced severe drought. These drought periods have increased reliance on groundwater. This causes groundwater levels to drop drastically, in return causing reduced water supply, land subsidence, seawater intrusion, and increased costs of pumping. In 2016, California passed the Sustainable Groundwater Management Act (SGMA) in order to balance levels of groundwater use and recharge. The law requires that local agencies in regions that are dependent on groundwater halt overdraft and develop plans to balance between pumping and recharge (DWR, 2021).

Some of the ways to find this balance is through recharge and by increasing groundwater recharge storage capacity. Artificial recharge methods include recharge basins, injection wells, and flooding to help increase groundwater levels (Todd & Mays, 2005). To increase groundwater recharge storage capacity, the method of constructing a subsurface dam can be applied to decrease subsurface travel times of water. To find the best recharge and storage enhancement option, some questions need to be considered, including:

1.) What is the most effective recharge method for this aquifer?

2.) Where in the site would be most effective for recharge?

3.) Where would a subsurface dam be most effective?

4.) What combination of different methods would be most effective?

A groundwater model that can represent the groundwater system in an area of interest is one of the most effective ways to answer these questions. The objective of this study is to develop a groundwater model for a site within the Santa Rosa Creek Watershed, near Cambria, California, to analyze the impacts of an existing recharge basin as well as to evaluate the effects a subsurface dam would have on the groundwater storage in the area of interest.

1.1 Background

The area of interest in this study will be called the Ranch and is within the middle reach of Santa Rosa Creek (SRC) Watershed, outside Cambria, California (Figure 3). Santa Rosa Creek is divided into three different reaches based on the geomorphology, land-use, and stream flow conditions: upper reach, middle reach, and lower reach. The middle reach mainly consists of farming (Stillwater Sciences, 2021). Specifically, on the Ranch, lemon and avocado trees. The owner of the Ranch relies on groundwater for irrigation of crops and for domestic use. The Santa Rosa Creek, which borders the southern boundary of the Ranch, could be gaining groundwater flow from the site, especially during dryer summer months. During periods of drought, the groundwater level drops and could limit the amount available for pumping as well as discharge to the creek. Creek Lands Conservation (CLC), a not-profit whose mission is to conserve and restore aquatic ecosystems along California's Central Coast, is identifying key projects and strategies to help enhance stream flow along the Santa Rosa Creek during dry season for steelhead (Oncorhynchus mykiss) rearing habitat (Stillwater Sciences, 2021).

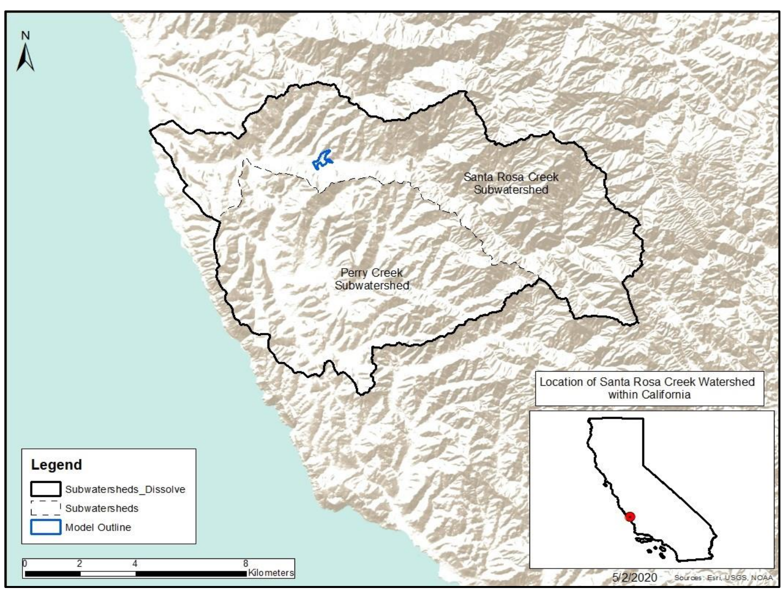

Figure 3: The Ranch Groundwater Model Outline within Santa Rosa Creek Watershed (Murray, 2020).

1.1.1 Santa Rosa Creek Watershed

The 48 mile^2 watershed is located in the southern portion of the California Coastal Range in northern San Luis Obispo County (Stillwater Sciences et. al., 2012). Bordering the east of the watershed is the Santa Lucia Mountain range and to the west is the Pacific Ocean. The topography is typical of the coastal region in this area with steep upland areas and low gradient valley bottoms bordering lower reaches (Figure 4).

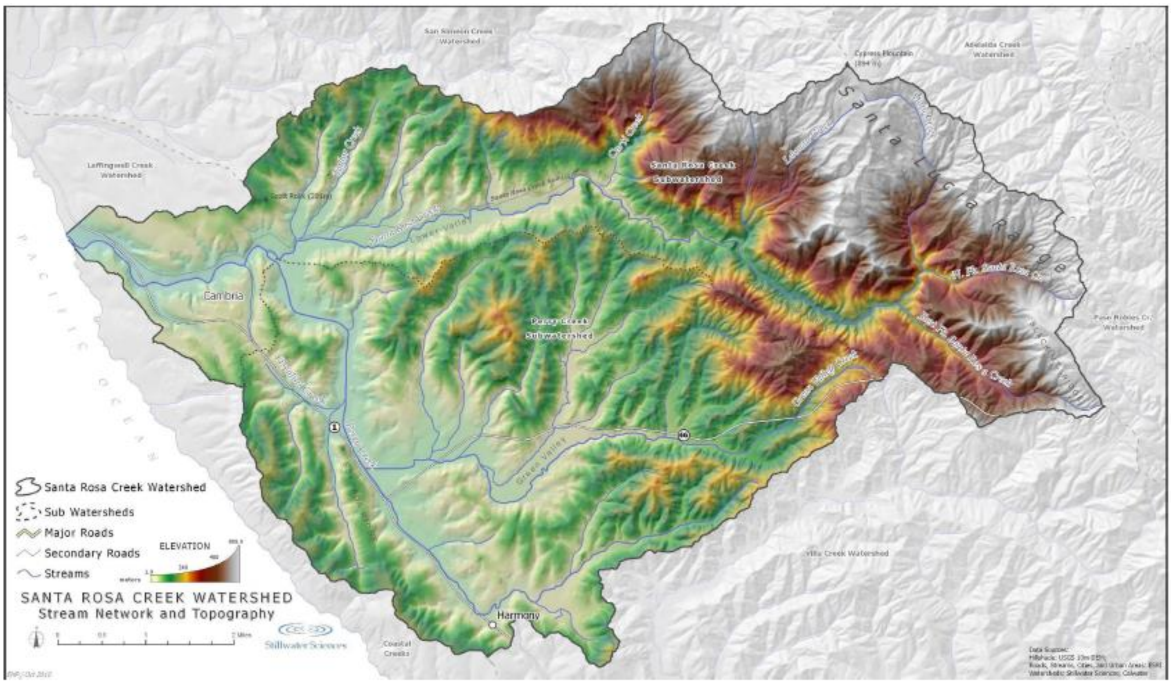

Figure 4: Santa Rosa Creek Watershed Stream Network and Topography (Stillwater Sciences et. al., 2012)

1.1.2 The Ranch

The area of the Ranch that is being modeled is a 126.2-acre farm site within the Santa Rosa Creek watershed (Figure 5). To the north lies steep hills and to the south, the Santa Rosa Creek. The east and west boundaries were defined by the hills on the northeast and northwest, and extensions of the hills on the southeast and southwest. As shown in the raster in Figure 6, there are moderate hillslopes in the northern area (red areas) of the Ranch but flattens in the southern areas (green areas). The lower areas of the site are used for agricultural purposes such as lemon and avocado trees. Starting in the northern region of the site, an ephemeral waterway runs through the middle of the site. In the northern middle region of site lies an existing recharge basin (Figure 5). The basin is roughly 0.2 acres and consists of a silty sand material lining the bottom.

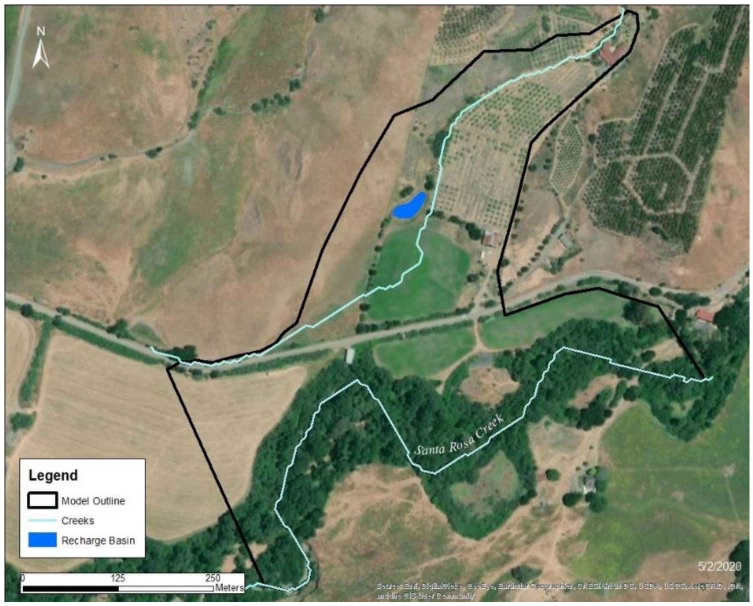

Figure 5: Farm Site Groundwater Model Outline with Creeks and Recharge Basin (Murray, 2020)

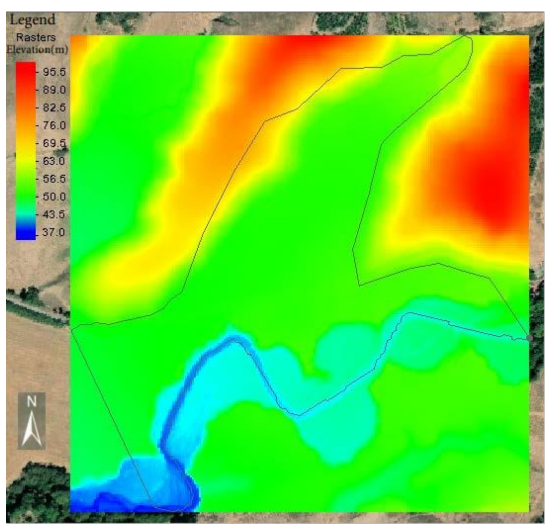

Figure 6: Elevation Map of the Ranch Site with Model Outline

1.1.3 Agricultural

Along the middle reach of the Santa Rosa Creek, there are roughly three dozen riparian parcels that are agricultural lands (Stillwater Sciences, 2021). The crops within this region that have the highest irrigation requirements include avocados, citrus, grapes, hay, and peaches. Avocados are a very high-water use crop, requiring 827 mm/yr of water during a typical year (Cal Poly SLO, 2021), and account for over half of the crops in the middle reach water use. Other hay and non-alfalfa crops account for roughly a quarter of the crops in the middle reach and require 1078 mm/year of water. Citrus is the next largest crop use and requires 848 mm/year of water. These three highly water intensive crops are mainly irrigated through the use of groundwater, which causes a strain on the groundwater aquifer in the Santa Rosa Creek watershed.

1.1.4 Creek Habitat

The Santa Rosa Creek used to have the largest population of steelhead trout (*oncorhynchus mykiss irideus*) along the central California coast, but in recent observations there has been a decline (National Marine Fisheries Services, 2006). Steelhead trout is listed as a threatened species under the Federal Endangered Species Act and is a California Department of Fish and Wildlife species of concern. Downstream of the middle reach, the creek becomes dry during summer months due to groundwater pumping and diversions, which can be detrimental to the steelhead trout population within the creek (Yates and Van Konyenburg 1998, D. W. Alley & Associates 2008, Nelson et al. 2009). Artificial recharge can help instream flows during these dry summer months and can enhance biotic conditions within the creek.

1.2 Purpose and Objectives

The purpose of this study is to expand upon a thesis conducted by Alex Murray in 2020. Murray’s purpose was to define and model, on a small scale compared to a work done by Dr. Muleta, a groundwater model to understand the effects of an existing artificial groundwater recharge basin at the farm site and further evaluate potential for other artificial groundwater recharge methods on the Ranch (Murray, 2020). This study will add to and refine to the existing model to verify and strengthen the findings in Alex Murray's research. This study also analyzes the effects of a proposed vertical subsurface barrier or "dam". The hopes of the proposed subsurface dam is that it will increase subsurface travel times of groundwater, and during the dry season an engineered pathway through the dam can optimize travel times for flow enhancement for the Santa Rosa Creek. By delaying the timing, it is thought a perched aquifer can form on top of the aquitard and slowly seep into the confined aquifer as well.

Throughout this study, GMS 10.4 was used for the groundwater modeling process. GMS 10.4 is a widely used groundwater modeling software (Aquaveo, 2019). This study used the existing 3 layers and 2m horizontal grid resolution that Murray incorporated into his model. The reason for creating this model was to develop a more detailed model compared to Dr. Muleta's 30 m resolution model for the Ranch.

CHAPTER 2. LITERATURE REVIEW

2.1 Previous Work

USGS conducted a three-year water resources study in 1998 and published a report concerning the hydrogeology, water quality, water budgets, and simulated responses to hydraulic changes in Santa Rosa Creek and San Simeon Creek groundwater basins (Yates & Van Konyenburg, 1998). The report stated that the basins are underlain by thin and narrow groundwater basins that supply nearly all the water for the area. Digital groundwater models were developed to investigate the effects of pumping and droughts. It was found that an increase in irrigation by farmers could lower groundwater levels by 10 feet and possibly cause subsidence in the lower Santa Rosa Creek Basin. It was also found that more recharge occurs in the Santa Rosa Creek groundwater basin compared to the San Simeon Creek groundwater basin.

Stillwater Sciences, Central Coast Salmon Enhancement, and Greenspace prepared the Santa Rosa Creek Watershed Management Plan in 2012 for the California Department of Fish and Game (Stillwater Sciences et. al. 2012). This plan discusses the natural, physical, and ecological trends in the watershed to forecast future watershed conditions, so recommendations can be made to improve the overall watershed aquatic habitat.

In 2017, Creek Lands Conservation (CLC) received a grant from the Wildlife Conservation Board (WCB) Stream Flow Enhancement Program to identify strategies and projects that measurably enhance spring and summer/late fall dry season stream flows in Middle Santa Rosa Creek (Stillwater Sciences, 2021). In this ongoing project, the project team includes the Upper Salinas-Las Tablas Resources Conservation District (US-LT RCD), a consulting team (Stillwater Sciences, Watershed Progressive, and Cleath-Harris Geologists), Hicks Law (Attorney at Law), and California's Polytechnic State University at San Luis Obispo (Cal Poly). The team is working to design engineering projects to measurably enhance spring and summer stream flows and increase aquatic habitat complexity.

Owen Cancroft and Alec Carroll performed a geophysical analysis of the Ranch and Santa Rosa Creek in 2019 (Cancroft and Carroll, 2019). They analyzed and interpreted geophysical surveys that were used to observe the subsurface aquifer at the Ranch and near the Santa Rosa Creek. Three geophysical surveys were conducted that included a seismic refraction survey, 2D Electrical Resistivity Tomography (ERT), and 3D ERT survey (Figure 7). The surveys found a sand and gravel matrix with Franciscan Mélange boulders and a discontinuous clay layer. From the 3D ERT survey (Figure 8) it was also found that there is an area of high resistivity that suggests boulders from the Franciscan Mélange complex or deposits of sand and gravel. If these areas are sand and gravel, then these areas would be productive when recharging an aquifer. The blue areas of Figure 8, show areas of low resistivity, such as clay or an impermeable layer.

Figure 7: Three Survey Sites on the Kendall Site (Cancroft, Carroll, 2019)

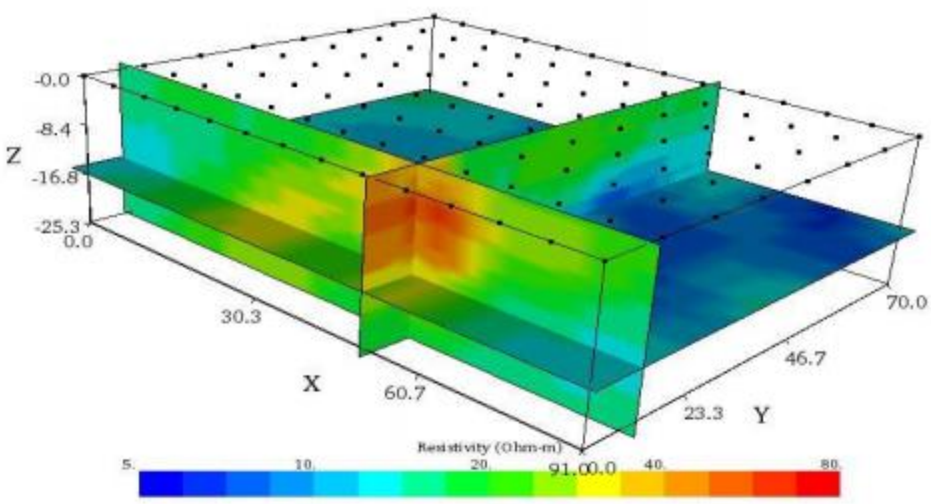

Figure 8: 3D ERT Survey Showing Resistivity Levels (Cancroft, Carroll, 2019)

Cleath-Harris Geologists prepared a technical memorandum for Creek Lands Conservations in 2019 discussing the Hydrogeology of the Middle Reach Santa Rosa Creek Valley (Cleath, 2019). The memorandum used historic data sources and investigations to provide the hydraulic characterization of the middle reach of the Santa Rosa Creek. Cleath-Harris Geologists provided a geologic cross section of the Ranch (Figure 9). Alluvial deposits that consisted of clays, sands, and gravels were found to be resting on the Franciscan bedrock. From the 3-D resistivity survey, it was interpreted that in the eastern side of the surveyed site there is an area of higher resistivity geologic unit and the high resistivity alluvial deposits become shallower on the upper portion of the valley. A pumping test was also performed at the irrigation well on the Ranch. The water levels in the monitoring well changed during the test, indicating groundwater connection between the monitoring well and irrigation well (the stream).

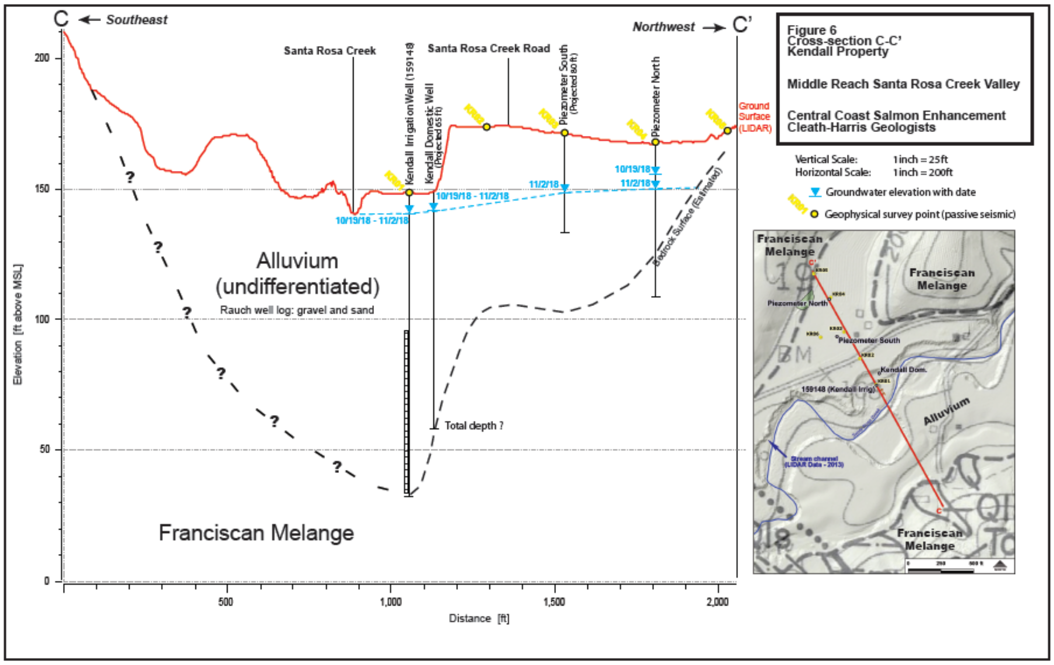

Figure 9: The Ranch Cross Section Showing Ground Surface, Alluvium, and Bedrock (Cleath, 2019)

Direct-push exploratory borehole drilling was conducted in 2019 at the Ranch as a preliminary part of the Santa Rosa Creek Flow Enhancement Pilot Project to obtain an understanding of the shallow subsurface and to evaluate percolation associated with proposed groundwater recharge (Malama et al., 2019). Seven exploratory boreholes were drilled that ranged in depths from 20 to 40 feet. Malama et al. (2019) observed that percolation methods for recharge at the site “would be challenging due to the presence of the near-surface low permeability subsurface unit” (Malama, Solum, & Nicholson, 2019).

Alex Murray, in 2020, prepared a thesis discussing his research on a groundwater model within the Ranch (Murray, 2020). His model focused on the impacts of an existing recharge basin on the groundwater aquifer storage. The model was calibrated to known groundwater levels throughout the site. Murray (2020) observed that the recharge basin does not percolate into the underlying groundwater aquifer because of a low hydraulic conductivity confined aquifer in the northern section of the site and a confining clay layer underneath the unconfined top layer. He recommended further data collection to help improve the model and to verify and strengthing his findings. It was also recommended that additional work and research be conducted to investigate possible recharge in the southern areas of the Ranch.

In November of 2020, Geosolutions completed two drill holes (B1 and B2) on the Ranch to obtain a deeper understanding of the subsurface hydrogeology. Figure 10 shows the new additional boreholes and the previous boreholes conducted by Malama et al. in 2019. These boreholes reached greater depths than the ones previous drilled on the site. Soil samples were taken from the site as well in order to conduct further research on the hydraulic properties of the soil. Creek Lands Conservation hydrologists created cross sections from these new additional boreholes, previous boreholes, and seismic survey conducted on the site (Figure 11,Figure 12,Figure 13).

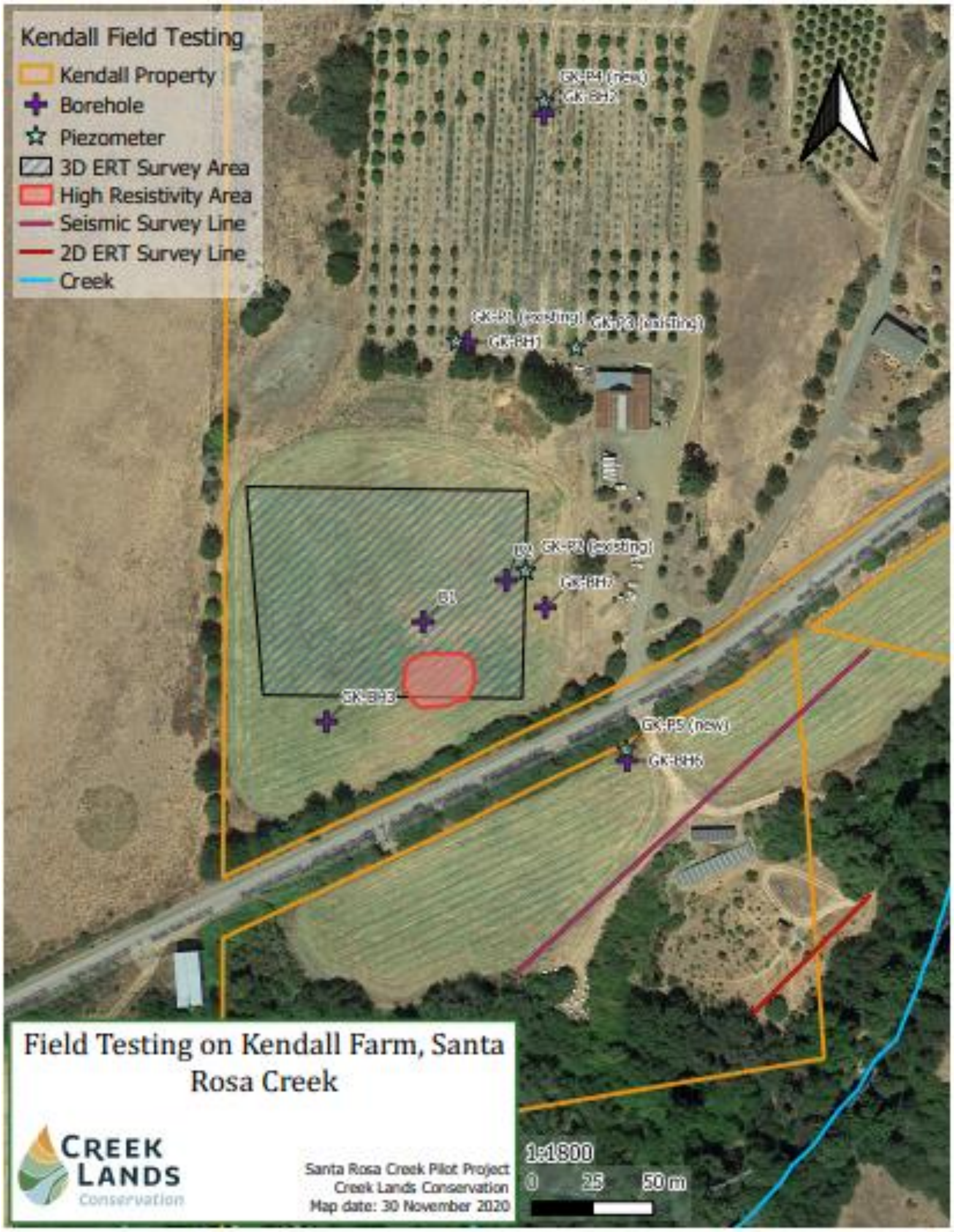

Figure 10: The Ranch Borehole Locations (CLC, 2020)

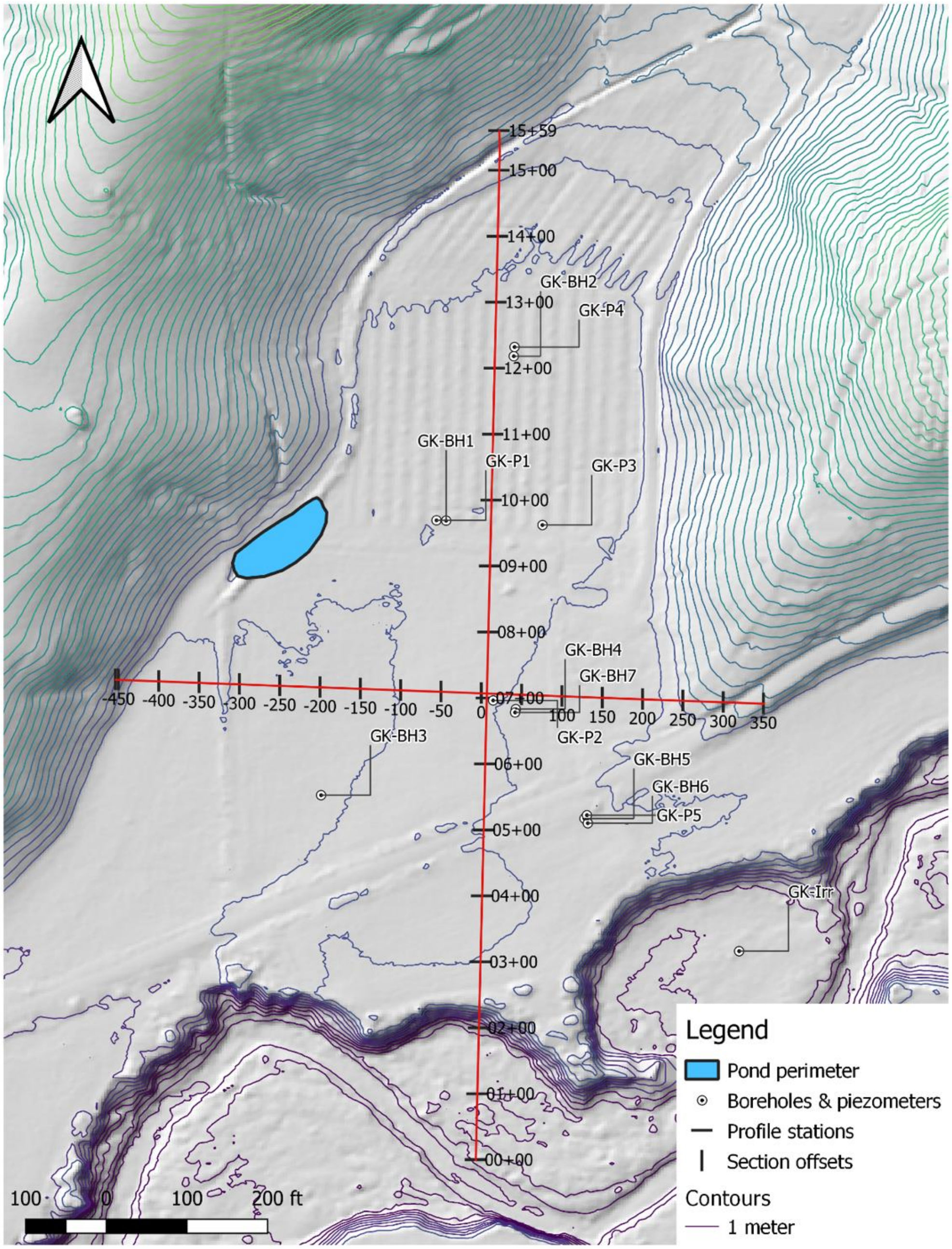

Figure 11: Cross Section Map of The Ranch Showing Cross-Valley (Cross Section D-D’) and Up Valley (Cross Section E-E’) (CLC, 2021)

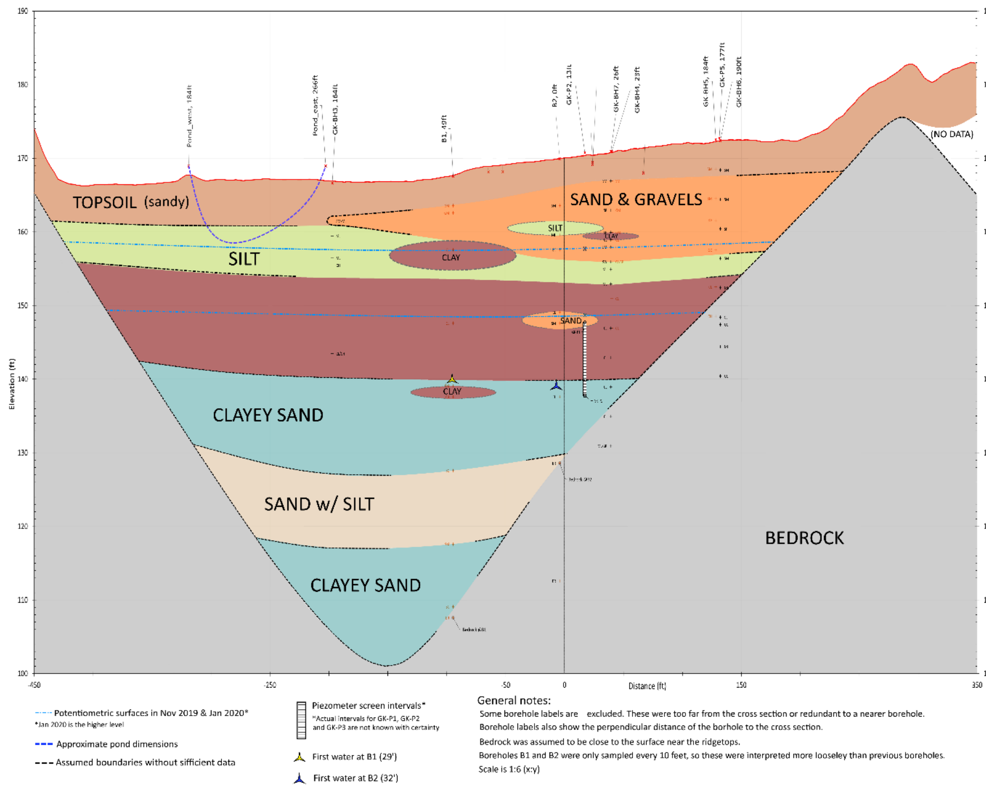

Figure 12: Cross Valley Cross Section (Cross Section D-D') (CLC, 2021)

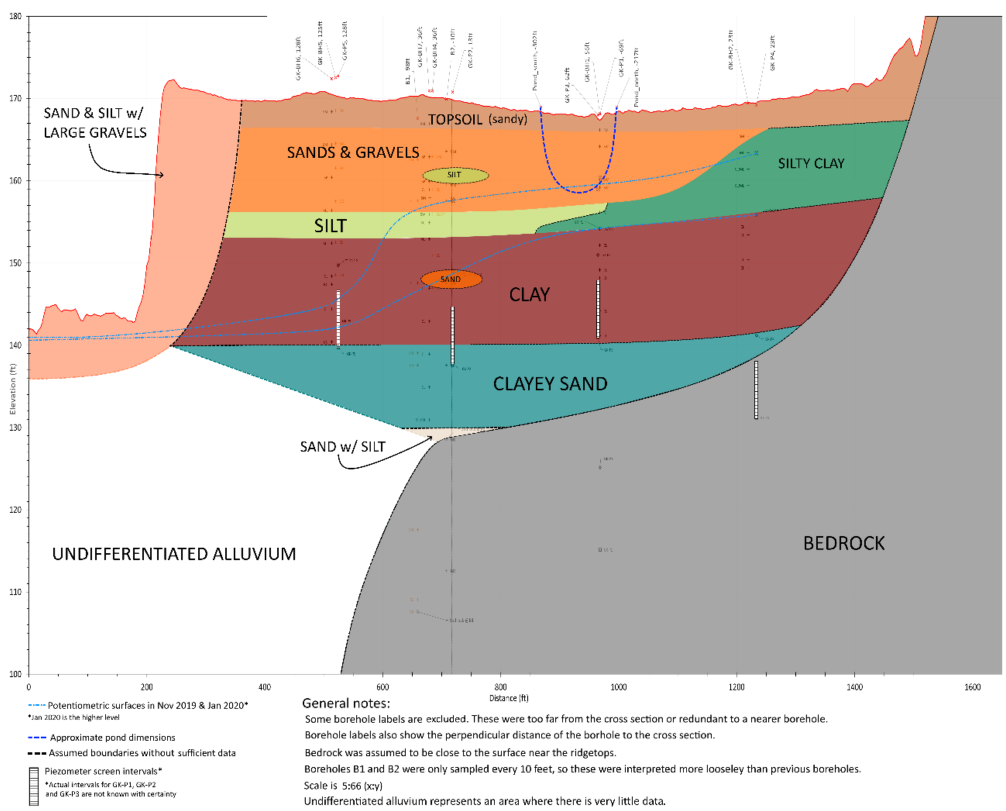

Figure 13: Up Valley Cross Section (Cross Section E-E') (CLC, 2021)

Dr. Muleta is conducting on-going work on a combined groundwater and surface water model of the entire Santa Rosa Creek Watershed (Muleta, 2021). The work is being performed alongside Creek Lands Conservation in an attempt to understand how and if artificial groundwater recharge can help streamflow in the watershed for steelhead trout and for groundwater supply for farmers within the watershed. Data from this model is being used to help develop the model in this investigation. This model developed in this study is on a much smaller spatial scale and more detailed in resolution compared to Dr. Muleta's 30 m by 30 m grid cells with two vertical layers. The two vertical layers represent a top unconfined layer and a bottom, potentially water-bearing, confined layer.

2.2 Artificial Groundwater Recharge

A method of controlling the declining groundwater is through artificial recharge, which is the practice of increasing the amount of water that enters an aquifer through engineered efforts (USGS, 2021). Some typical recharge methods include: surface basins, excavated basins, trenches, shaft wells, and aquifer wells (Figure 14).

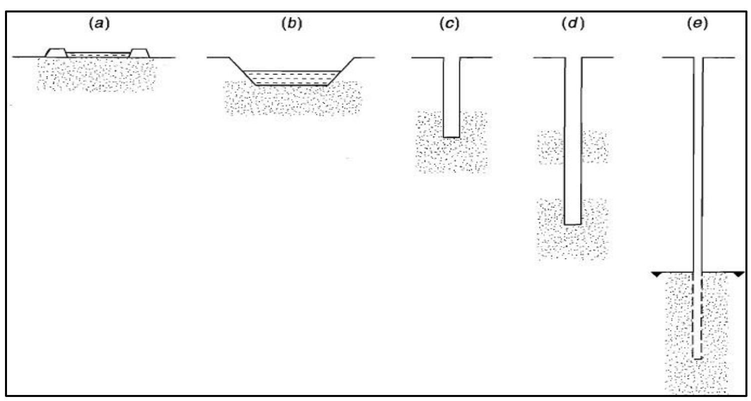

Figure 14: Artificial Groundwater Recharge Methods (a) surface basin, (b) excavated basin, (c) trench, (d) shaft well, (e) aquifer well. (Bouwer, 1999).

Basins are helpful in areas where the aquifer is closer to the surface, while wells are more efficient for confined aquifers that are deeper in the subsurface. The artificial recharge method this study will focus on is an excavated recharge basin since the site already includes one.

2.2.1 Recharge Basin

A recharge basin is a widely used method of artificial groundwater recharge. These basins are artificial ponds that are designed to infiltrate water into groundwater aquifers below the surface. These basins do not release water except through infiltration, evaporation, or during flood conditions (Todd & Mays, 2005). Recharge basins must be carefully designed to infiltrate the soil on the site at a rate to not cause flooding. They may be less effective if the groundwater levels are too high, the soil is too compacted, there is high levels of sediment in the water, or if there is a high clay content. Shallow basins where the water depth is about 10 to 30 cm are the most desirable to sustain high infiltration rates and to promote ease of maintenance for maximum hydraulic loading. The recharge rate of typical basins varies from 30 m/year to 300 m/year based on the hydraulic conductivity of the soils, groundwater levels, quality of water infiltrating into the basins, climate, and recreational or environmental constraints (Bouwer & Rice, 1989).

2.3 Subsurface Barrier

A subsurface barrier, or dam, helps store groundwater in the pores of strata and uses groundwater in a sustainable way (Ishida, 2010). They are used in a sustainable way by preserving land from being submerged with a reservoir and there is no danger for a potential dam break that surface water reservoirs have. There are many advantages when it comes to a subsurface barrier compared to a surface dam. Underground dams are built across streams or valleys by digging a trench to bedrock and are composed of a cut-off wall, made of a clay or bentonite mixture, to dam the groundwater flow. These dams have been used around the world and can store a few hundred to several million cubic meters of groundwater depending on the size (Ishida, 2010). Some technical requirements and recommendations for the construction of an underground dam include: (1) Distribution of soil layers that have effective porosity and hydraulic conductivity to allow for groundwater flow; (2) The lower impermeable basement must be of low permeability; (3) The depth of the subsurface barrier to the impermeable basement is economically feasible; (4) There must be groundwater recharge to match the planned water amount for development; (5) There should be little impact on the lower catchment area (JGRC, 2006). Figure 15 shows a typical subsurface dam.

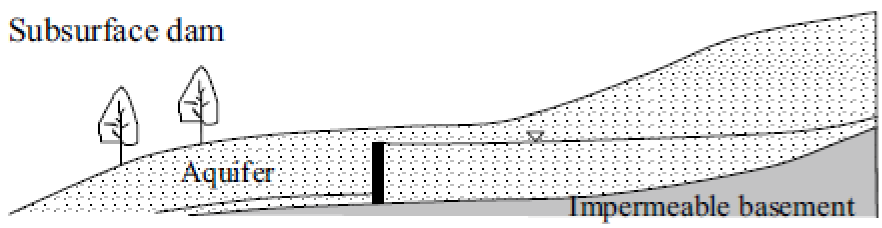

Figure 15: Subsurface Dam (Ishida, 2010)

CHAPTER 3. METHODS AND MATERIALS

This chapter discusses the data that was used in Alex Murray's groundwater model and additional data used in this study to expand upon the groundwater model.

3.1 Layers and Elevation

Three layers were used to represent the groundwater model. The topmost layer, layer 1, represents the topsoil on the site and is an unconfined layer. The middle layer, layer 2, is a confining layer or aquitard. The bottom layer, layer 3, is a confined layer. The elevations of the top of layer 1, which represents the ground surface were obtained from a LIDAR survey of the Santa Rosa Creek Watershed conducted by PG&E in 2013 (PG&E, 2013) (Figure 16).

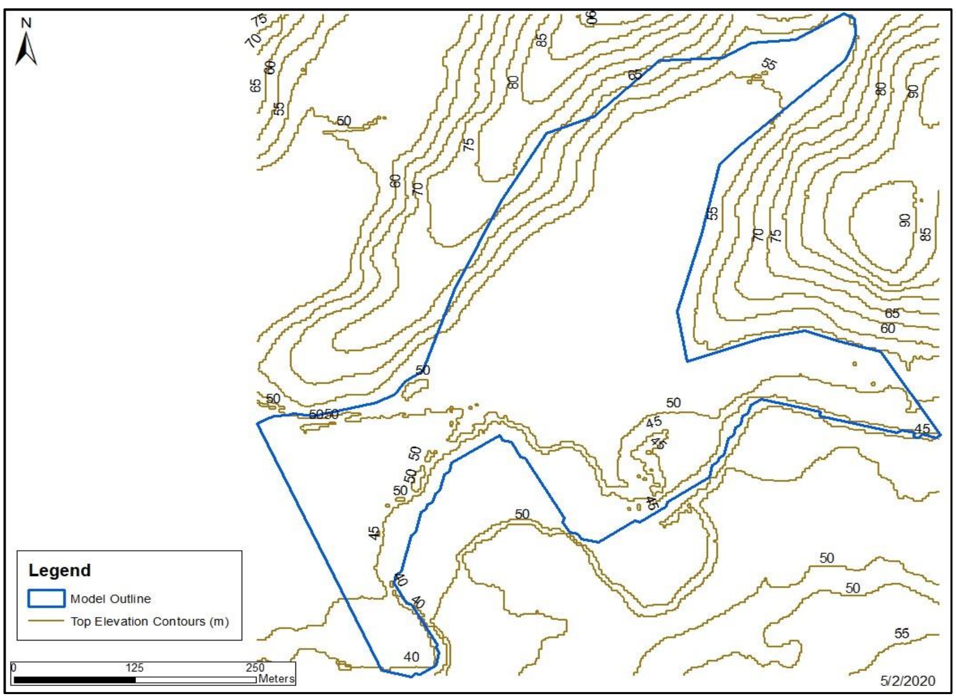

Figure 16: Top of Layer 1 Elevation Raster Clipped to GMS Model Outline and Converted to a Topographical Map (Murray, 2020)

The top of layer 2 elevations (bottom elevations of layer 1) were determined based off of geological cross sections from Creek Lands Conservation (Figure 11,Figure 12, Figure 13) (CLC, 2021). In the previous model the elevations were estimated to be a constant 5 meters below the top elevations of layer 1. The top of layer 3 (bottom of layer 2) was also determined using the geological cross sections from Creek Lands Conservation. In the previous model the elevations were again estimated to be a constant 5 meters below the top elevations of layer 2. This model is more detailed in the elevation variations between the top two layers because of additional information gained from Creek Lands. The bottom of layer 3, which represents the impermeable bedrock, was interpolated from the Tim Cleath Report by Dr. Muleta (Cleath, 2019) (Figure 17). The map was processed into a raster file and extended on the northwestern side to be able to include the whole outline of the site.

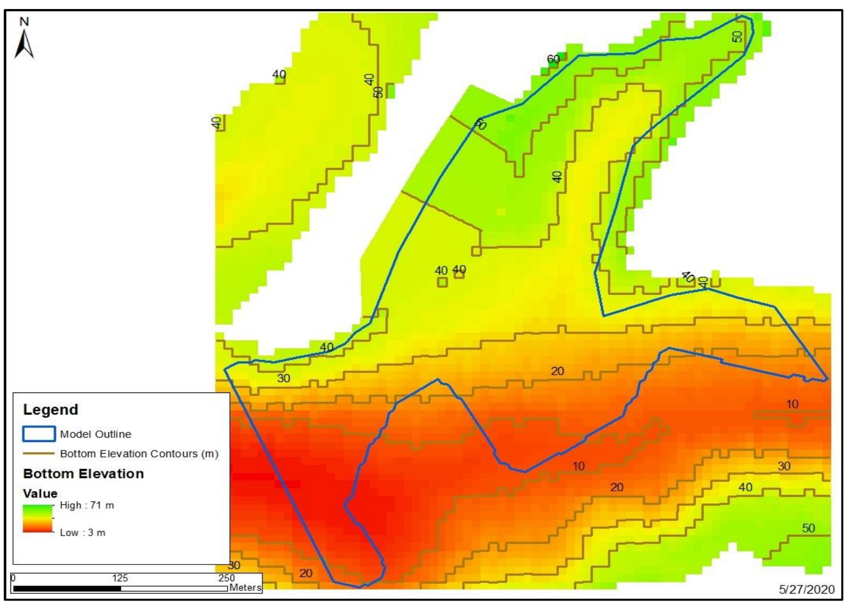

Figure 17: Bottom Elevations of Layer 3 with the Outline of the Area Being Modeled (Murray, 2020)

3.2 Variable Head Boundary Conditions

Three variable head boundaries exist in the model. These include the Santa Rosa Creek, which borders the southern boundary of the model, as well as the boundaries on the southeast and southwest of the model (Figure 18). These boundaries were necessary because this is where the model was cut from the larger Santa Rosa groundwater basin. The model however, doesn’t represent the interaction between the creek receiving flow/feeding flow from the aquifer, since the Santa Rosa Creek was modeled as a boundary and below the creek wasn’t modeled.

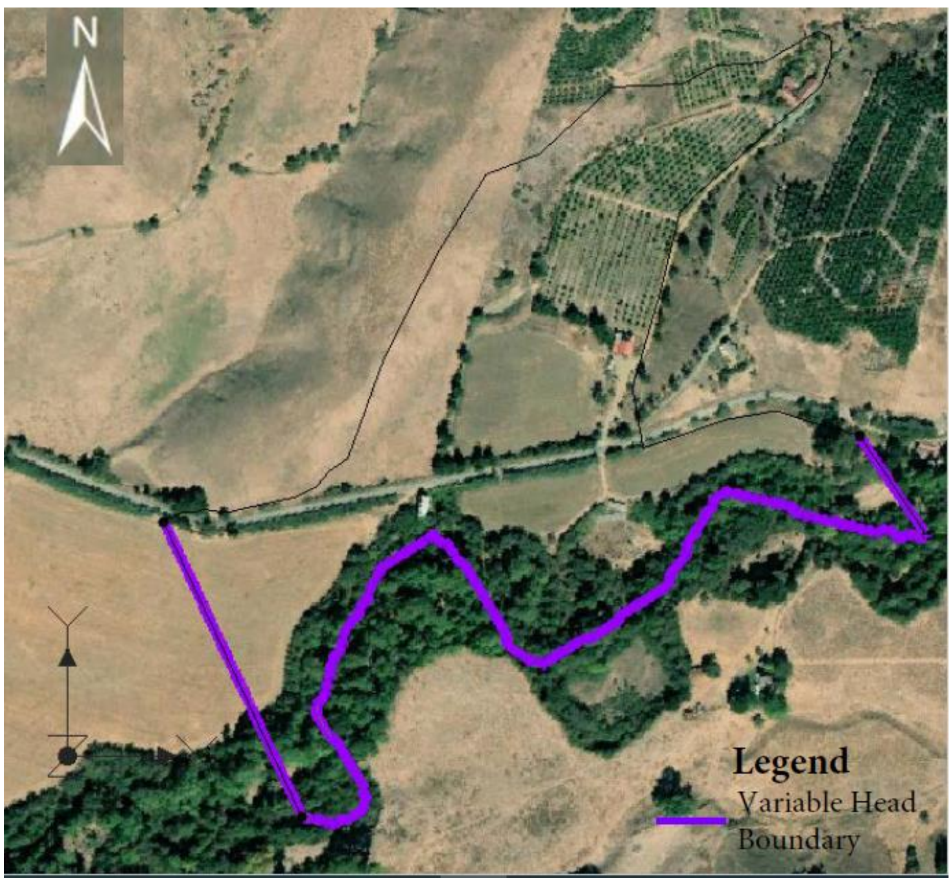

Figure 18: Variable Head Boundaries in Model

The northeast boundary represents groundwater flow flowing into the site, and the southwest boundary represents groundwater flow flowing out of the model. The variable heads within Santa Rosa creek were determined from daily depth values of the creek to the top elevations of layer 1 for a couple of different segments along the creek. These values were estimated based on seasonal averages. During the wet season, January through March, the maximum water elevation was 1.5 meters and declined in the dry seasons to 0.1 meters. To speed up the calibration and run times of the model, the daily data from the previous model was converted into monthly average data (Figure 19).

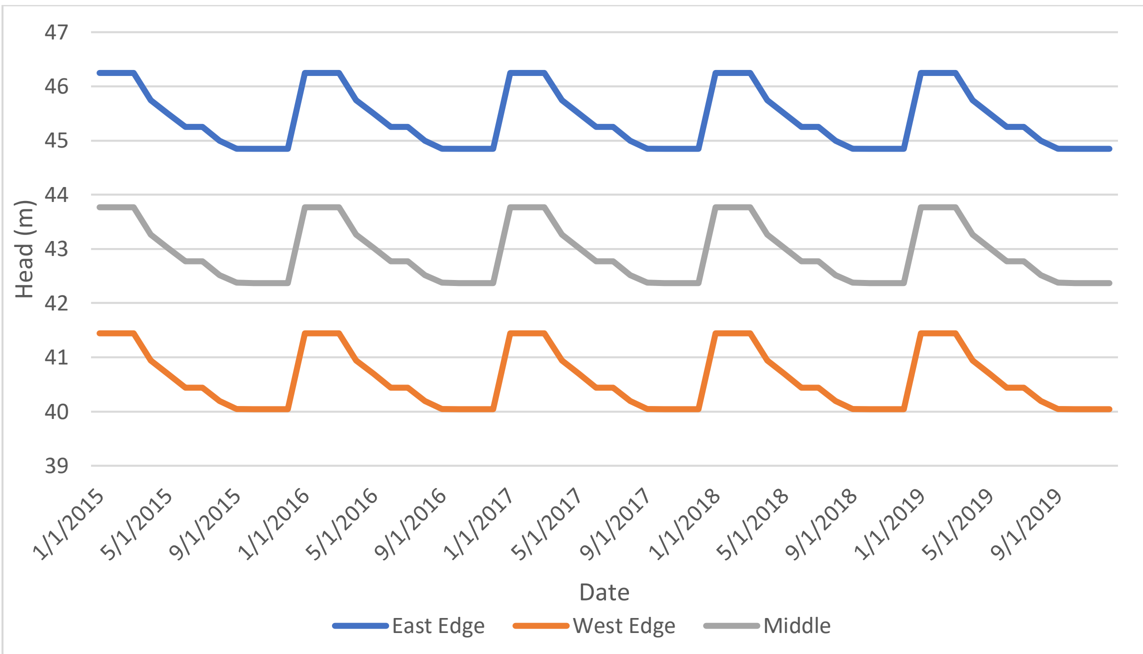

Figure 19: Monthly Data for Three Santa Rosa Creek Boundary Head Values

The variable head boundaries along the southeast and southwest boundaries were found using the Santa Rosa Creek heads at the east and west locations. A hydraulic gradient of 1% was assumed from north to south and heads along the northeast and northwest borders were able to be determined (Figure 20).

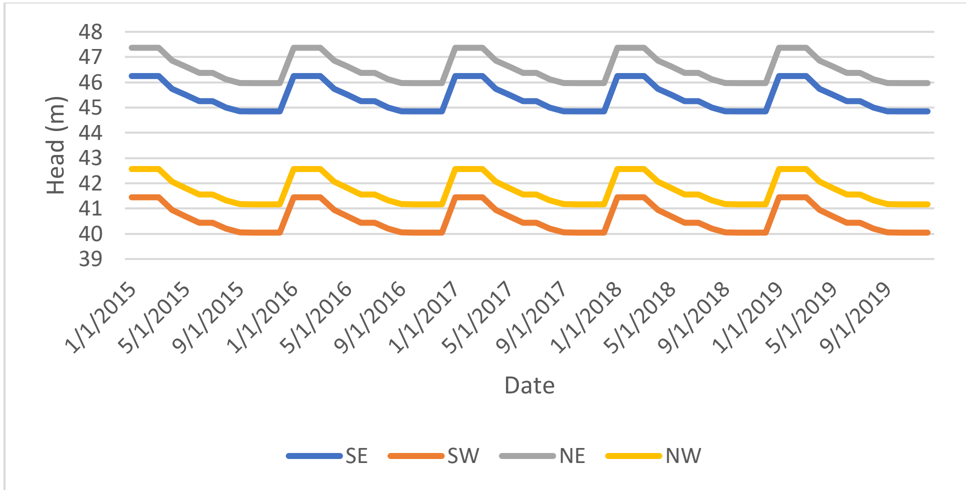

Figure 20: Monthly Average Heads for Variable Head Boundaries

3.3 Streams

Two streams are incorporated in the model for the Ranch. The shapefiles and data for the streams were provided by Dr. Muleta (Muleta, 2020). The two streams are an ephemeral channel that runs from the northeast side of the model to the southwest side of the model and the Santa Rosa Creek (Figure 21).

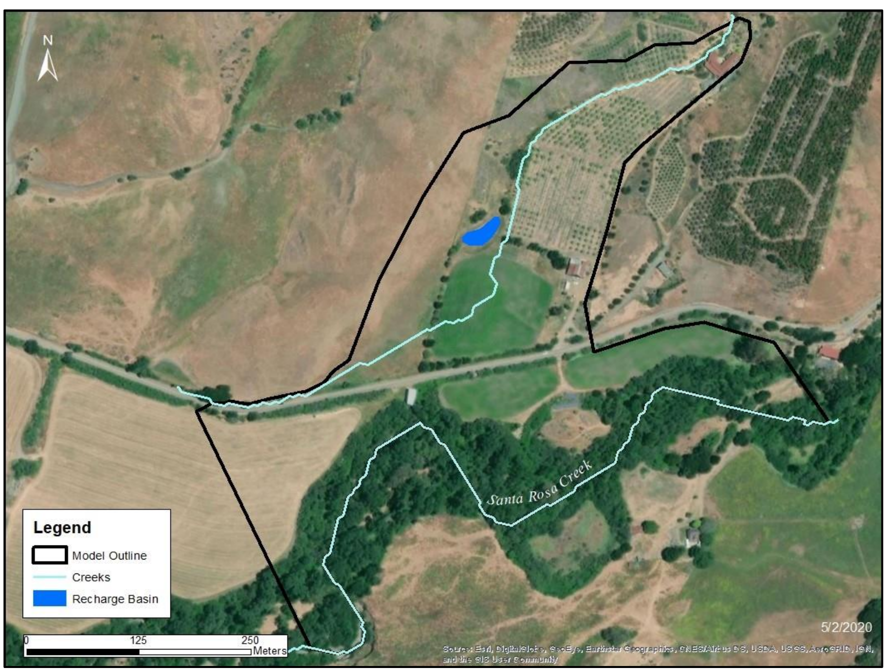

Figure 21: Ephemeral Stream and Santa Rosa Creek (Murray, 2020)

The data provided for the streams included stream conductance and daily streamflow data. Conductance, in units of length per time, within this model is the hydraulic conductivity of the stream bed divided by its thickness, all multiplied by the area of the river. The daily data for the ephemeral channel was converted into monthly data to reduce calibration and run time of the model (Figure 22). The streamflow data for the ephemeral channel was minimal due to it being dependent on storm events. On an average year the streamflow peaked in spring at around 200m^3/day, but during 2017 it rose to 1,300 m^3/day. The streamflow data for the Santa Rosa Creek was not used since it was modeled as a variable head boundary.

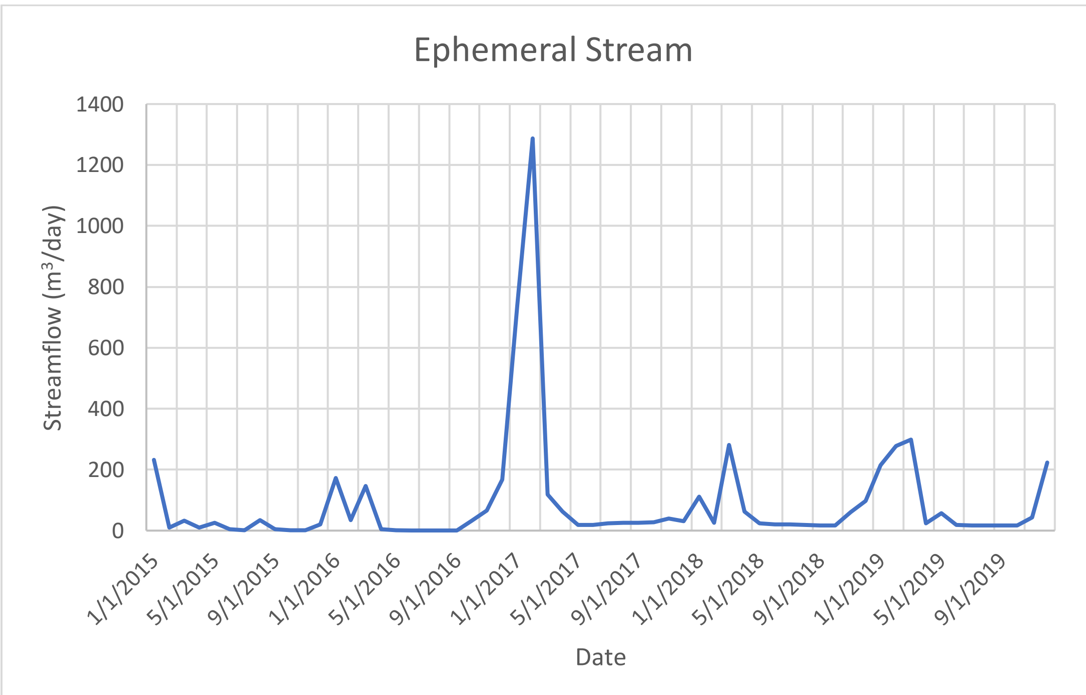

Figure 22: Ephemeral Stream Monthly Streamflow Data

The Ephemeral channel's sinuosity also needed to be calculated as an input into the model. This was done through the use of ArcMap and Equation 1.

$$Sinuosity = \frac{Length\ of\ Stream\ Channel}{Length\ of\ Straight\ Line\ Distance} \qquad \text{(Equation 1)}$$

3.4 Agricultural Well

Within the Ranch there is only one irrigation well located in the southern portion of the site (Figure 23). The well pumps from the third confined layer and the pumping rates were based off of crop evapotranspiration (ET) demand plus losses based on imperfect transmission or irrigation schedule (Watershed Progress, 2021). The irrigation water use was estimated to be 110% of ET, which represents minimal transmission losses. This assumption put water use at 3.0 acre-feet/acre per year. This value increased from Dr. Muleta's estimation of 2.7 acre-feet/acre per year (Muleta, 2021). Figure 24 shows the newly adjusted pumping rates due to the increase in estimated irrigation use. Pumping rates were also converted into monthly data to reduce calibration and run time of the model.

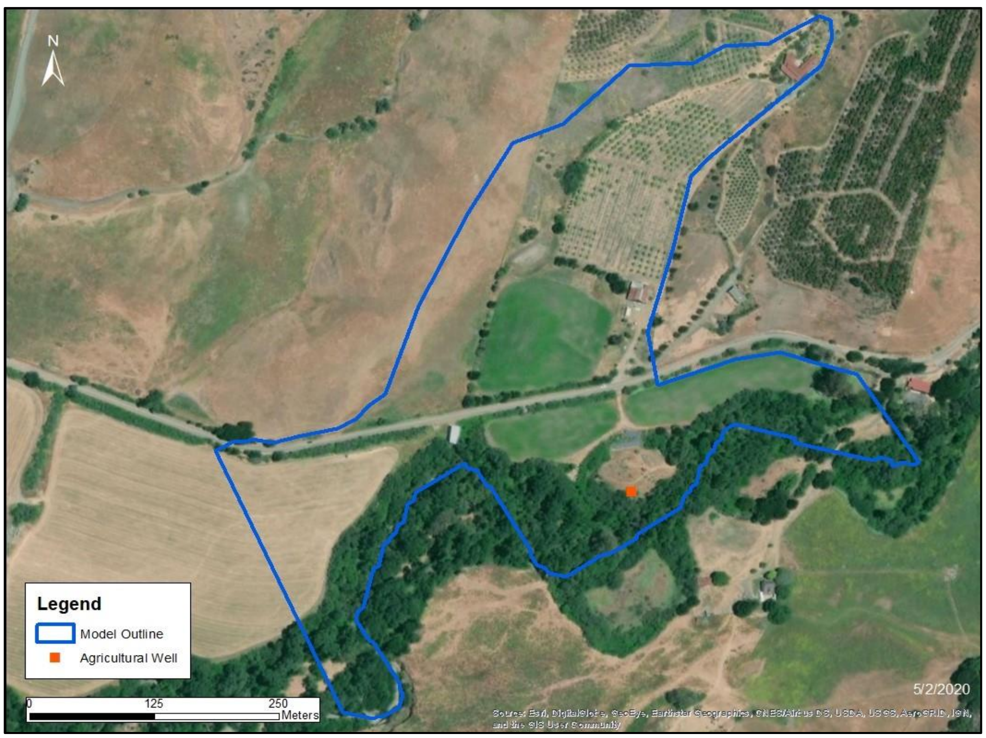

Figure 23: Location of Agricultural Well within the Model (Murray, 2020)

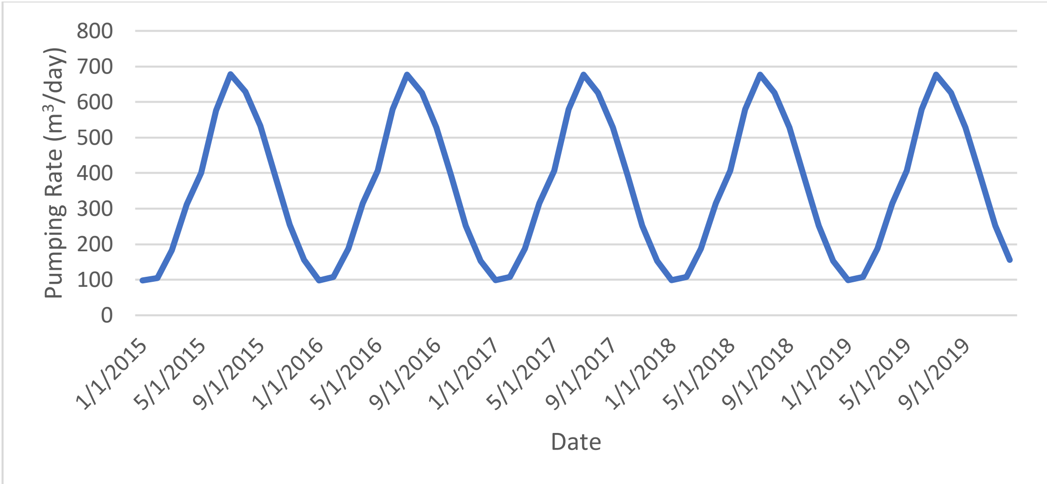

Figure 24: Monthly Average Pumping Rates for the Agricultural Well

3.5 Recharge

3.5.1 Sub-basin Recharge

The model was broken into four different sub-basins for recharge rates based off of Dr. Muleta's surface water model (Muleta, 2020) (Figure 25). Daily recharge rates provided from Dr. Muleta were converted into monthly average rates for each sub-basin (Figure 26). The recharge rates were greatest in July through September and decreased in the winter months from October through June. On average the recharge rate during its peak in the summer is $1.1*10^{-4}$ m/day and in the dry seasons $5.0*10^{-5}$ m/day. 2017 was a very wet year so this explains the large jump in recharge rates. The average for the wet months was $6.48*10^{-4}$ m day.

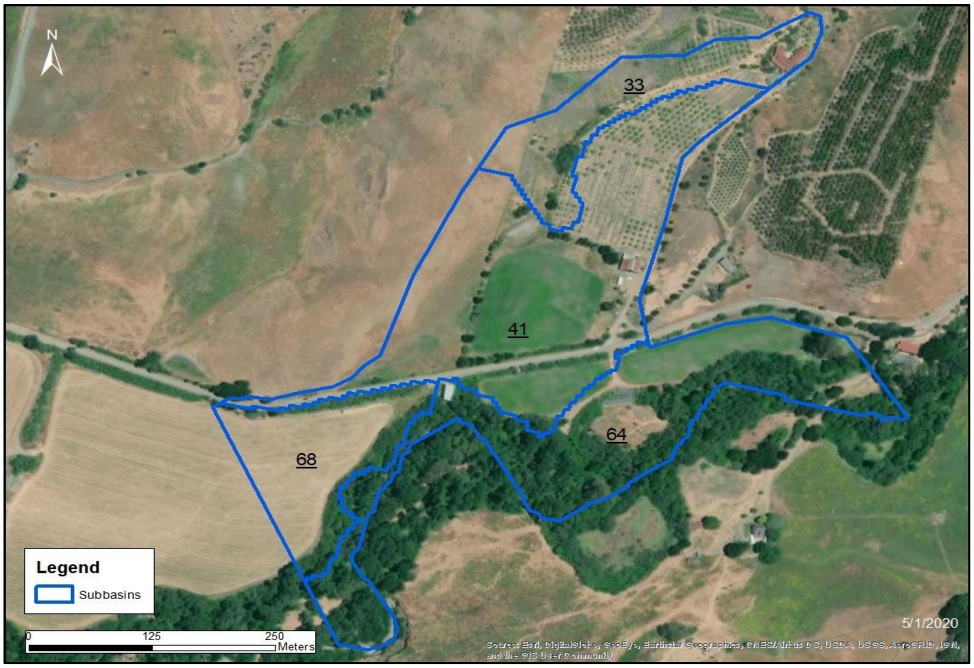

Figure 25: Map of Four Different Sub-basins within Model (Murray, 2020)

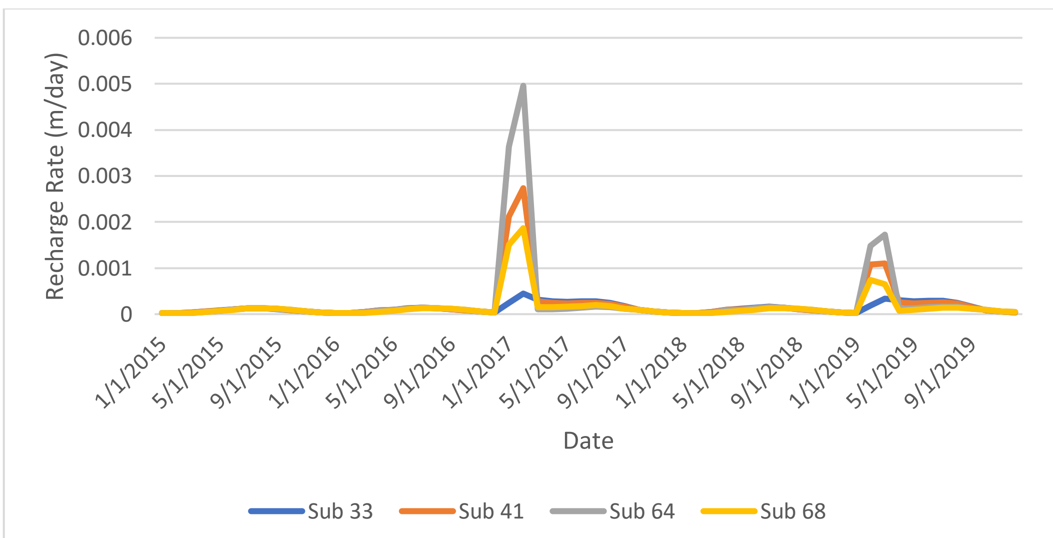

Figure 26: Monthly Average Recharge Rates of the Four Sub-basins in the Model.

3.5.2 Existing Recharge Basin

The existing recharge basin's, shown in Figure 21, recharge rates were estimated by Dr. Muleta based on the owner of the Ranch's recollection of filling and drying the basin and Dr. Muleta's surface water model's streamflow for the ephemeral channel. The owner also has a piezometric well that tracks that water levels in the basin that helped with estimation of the recharge rates. Figure 27 shows the monthly average of the recharge rate in the basin. The recharge occurred started occurring usually in February each year and stopped around May. The monthly averages per day were 0.1 m/day of recharge into the basin. The recharge basin at the Ranch is roughly 48 meters above sea level. Historic water level data shows that the water table ranges from 45 to 51 meters for a typical year. It is also noted that clogging isn't an issue at the site and the owner of the Ranch biannually cleans out the basin.

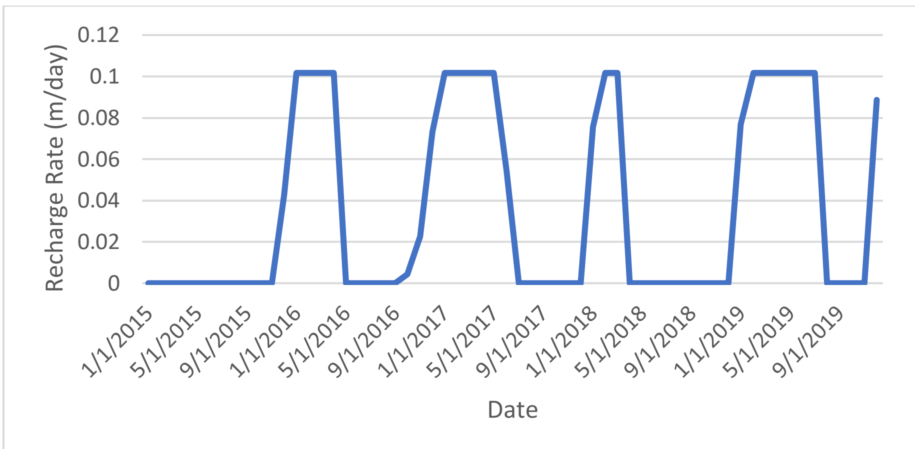

Figure 27: Recharge Basin Monthly Average Recharge Rates

3.5.3 Mountain Front Recharge

Mountain front recharge data was provided by Dr. Muleta for the northern boundary of the site where lateral subsurface flow from mountains to the valley aquifer exist (Figure 28) (Muleta, 2021). The amount of recharge is shown in Figure 29. The mountain recharge occurred usually from December to April over the five-year period. During 2016 and 2018 it averaged roughly only 0.019 m/day. In 2019 it increased to 0.064 m/day, and during the wet year of 2017 the average was 0.1 m/day.

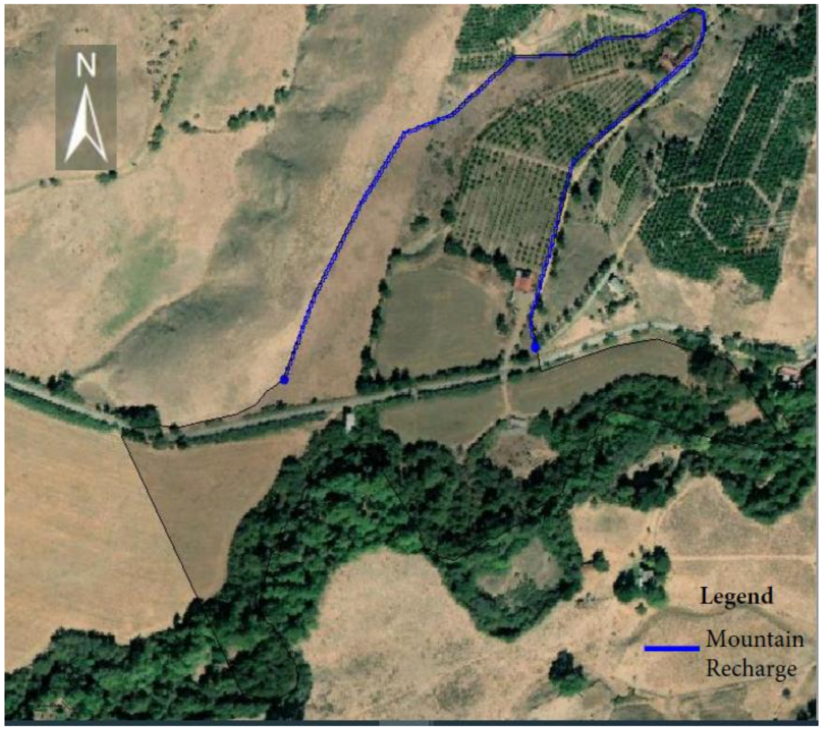

Figure 28: Location of Mountain Front Recharge on Northern Boundary

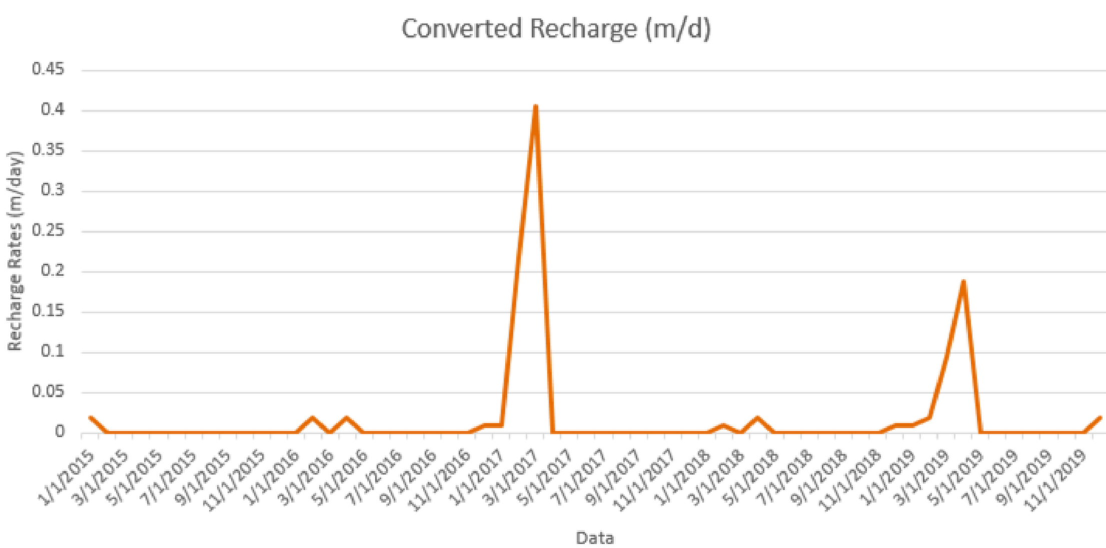

Figure 29: Monthly Average Mountain Front Recharge on Northern Boundary

3.6 Evapotranspiration Rates

Daily evapotranspiration rates that were provided by Dr. Muleta were converted to monthly averages (Figure 30) for each sub-basin shown in Figure 25. Evapotranspiration peaked in summer months at just over 0.002 m/day, and in the winter months decreased to $1.0*10^{-4}$ m/day on average over the five-years. It is assumed that evaporation was possible up 2 meters below the top of layer 1.

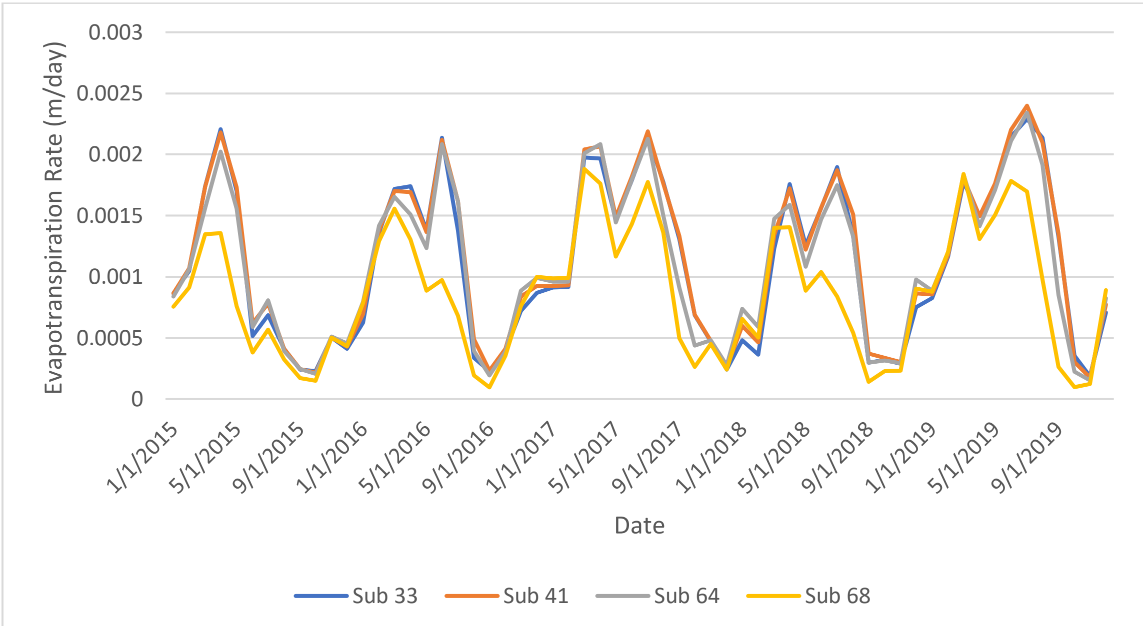

Figure 30: Monthly Average Evapotranspiration Rate for each Sub-basin

3.7 Observation Wells

Water level data was monitored at three different piezometric wells within the study area. These wells include KP1, KP2, and KP3 (Figure 31). The data for these wells was obtained from the owner of the Ranch (Figure 32). Water levels increased to roughly 49-52m during the wet months and decreased to 45-46m in the dry months. These well observations were used to help calibrate the model to make the model more representative of the groundwater system. The irrigation well (K2) has observation data from 1988-89 (Yates & Van Konyenburg, 1998). Although this data is from decades ago, the water levels could provide some insights about water levels in the vicinity of Santa Rosa Creek.

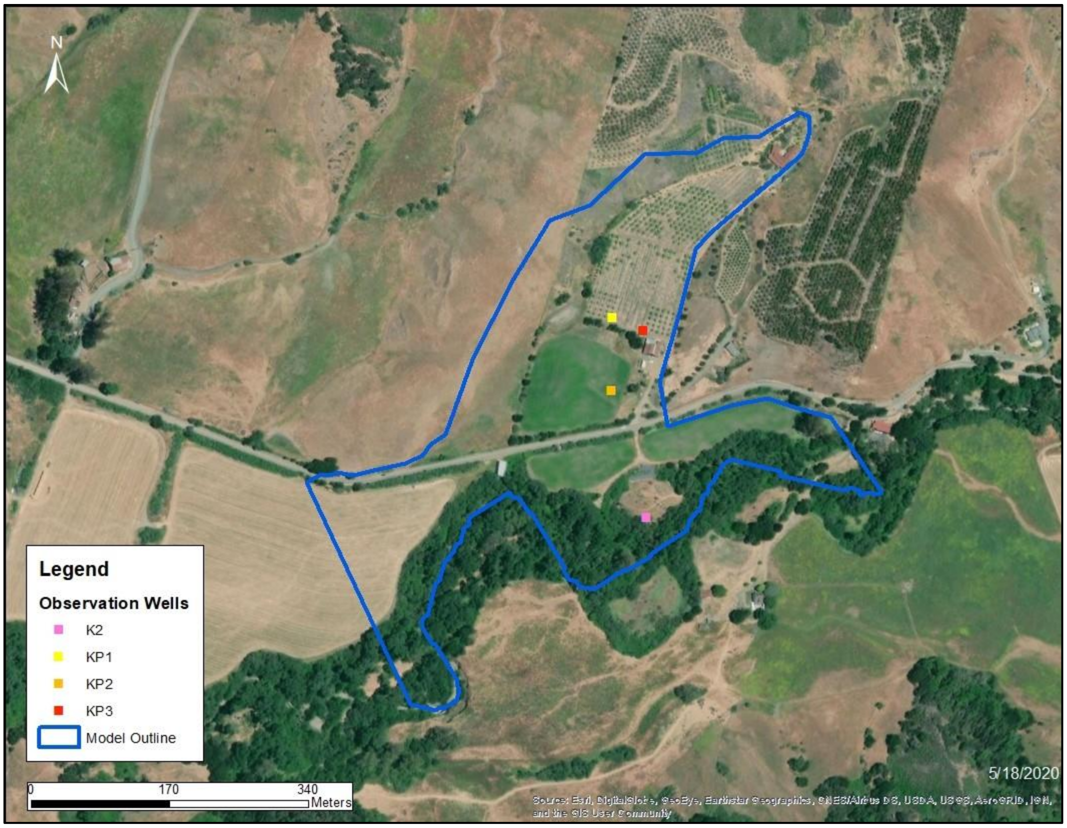

Figure 31: Map of Observation Wells and Irrigation Well in Model (Murray, 2020)

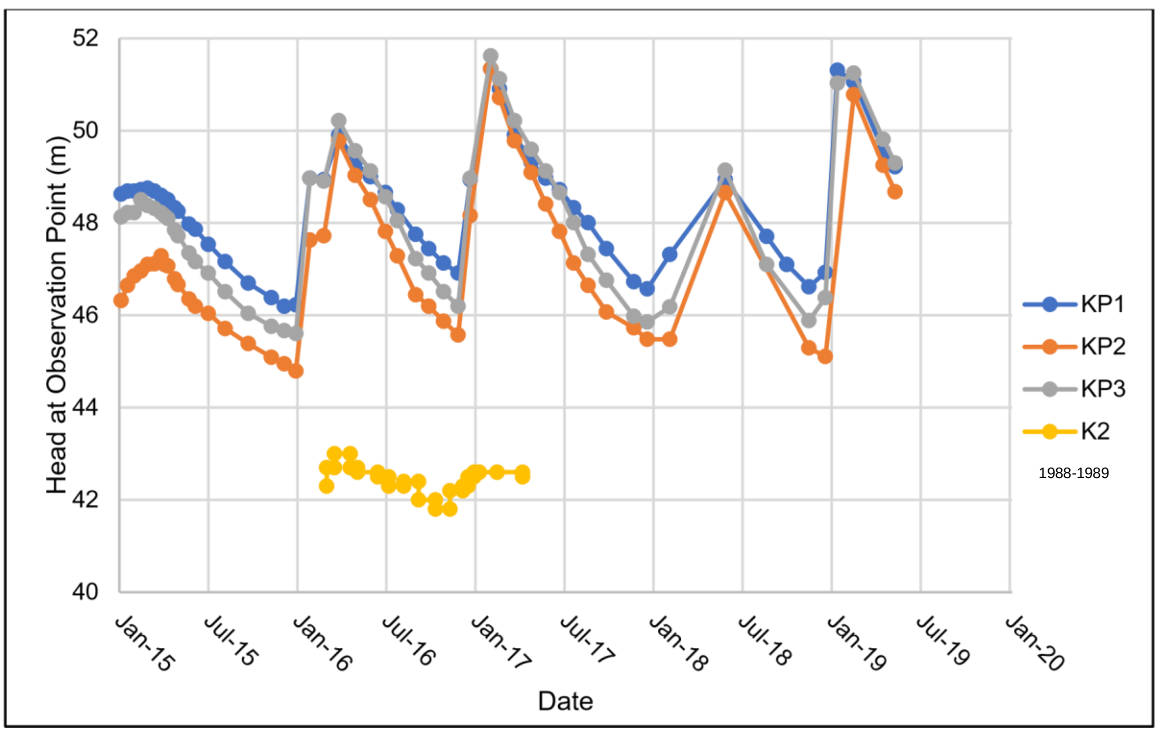

Figure 32: Head Data from Observation Wells

3.8 Field Data

Creek Land Conservation obtained field data from the Ranch which included soil samples from the addition of two new boreholes drilled in 2020 (B1 and B2) and soil logs for the boreholes. Samples from borehole B1 included samples from depths at 9, 43, 50, 60, and 70 feet below the ground surface. Samples from B2 included samples at depths at 9, 19, 39, and 49 feet. The samples were obtained for analysis at California Polytechnic University's Geotechnical Laboratory. The analysis will help understand the subsurface at the site to characterize the aquifer.

3.9 Lab Data

The samples obtained from the field were analyzed at California Polytechnic University's Geotechnical Laboratory with the help of Nephi Derbidge. The goals of the lab testing included characterizing the samples as well as finding the vertical hydraulic conductivities of a few representative samples. The tests used a variety of ASTM standards that include ASTM D1140 (ASTM International, 2017a), ASTM D2487 (ASTM International, 2017b), ASTM D5084 (Method C) (ASTM International, 2016), ASTM D5084 (Method F) (ASTM International, 2016), and ASTM D6913 (ASTM International, 2017c).

To find the vertical hydraulic conductivity of samples from B1 at 9, 43, and 50 feet, ASTM D5084 (Method F) was used. ASTM D5084 (Method F) is a constant volume-falling head (by mercury), rising tail water elevation. This method is used for samples that are expected to have low hydraulic conductivity values. The samples in bags were compacted into rings based on their depth and moisture content. The soil was extracted from the rings with a hydraulic press and a membrane was placed around the sample with porous stones and filter paper on top and bottom of the sample to allow for water flow. The sample was put into the permeameter cell, filled with water, pressurized to the effective stress desired and saturated for a couple days before the permeation tests were run (Figure 33). The falling head test included taking time measurements of different head losses across the sample as water was run through it for multiple trails.

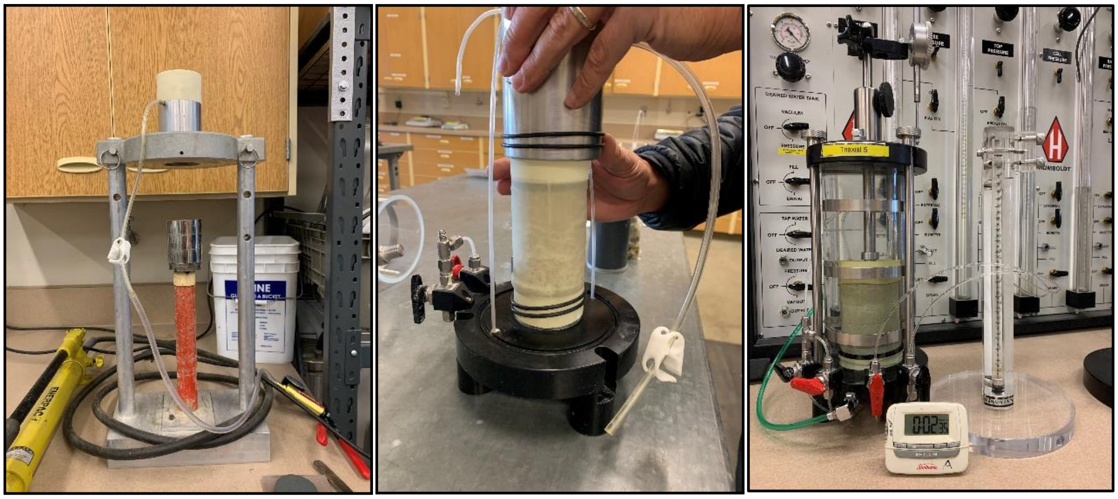

(a) (b) (c)

Figure 33: (a) Soil Sample in Rings being Extracted (b) Sample with Membrane Around it and Porous Stones on Top and Bottom (c) Permeameter Cell with Sample

To find the vertical hydraulic conductivity of the sample from the observed falling head and time measurements, Equation 2 was used.

$$k = \left(\frac{a_{in} \cdot a_{out}}{(a_{out} + a_{in})} \cdot \frac{1}{(G_{Hg} - 1)}\right) \cdot \frac{L}{A} \cdot \frac{1}{\Delta t} \cdot \ln\left(\frac{\Delta h_1}{\Delta h_2}\right) \qquad \text{(Equation 2)}$$

Where: k = hydraulic conductivity (m/s),

a_{in} = cross-sectional area of the reservoir containing inflow liquid (m^2),

a_{out} = cross-sectional area of the reservoir containing outflow liquid (m^2),

G_{Hg} = the ratio of the density of mercury to the density of water (specific gravity of mercury) at the test/trial temperature,

L = length of specimen (m),

A = cross-sectional area of specimen (m^2),

Δt = interval of time over which the flow occurs ($t_2 - t_1$) (s),

Δh_1 = head loss across the permeameter/specimen at t_1 (m),

Δh_2 = head loss across the permeameter/specimen at t_2 (m).

The hydraulic conductivity of samples B2 at 9 and 19 feet were found using ASTM D5084 (Method C). This method is similar to Method F, but this is a falling head test not over a constant volume with a rising tail water elevation and is for soils with an estimated higher hydraulic conductivity. The rest of the procedure is the same as Method F, but this method doesn't require a mercury reservoir and tubing. Equation 3 shows the calculation of hydraulic conductivity for Method C.

$$k = \frac{a_{in} \cdot a_{out} \cdot L}{(a_{in} + a_{out}) \cdot A \cdot \Delta t} \ln\left(\frac{\Delta h_1}{\Delta h_2}\right) \qquad \text{(Equation 3)}$$

Table 1 shows results of the five tests performed to determine the vertical hydraulic conductivity of the samples. Samples at 9 feet were obtained from the clay layer, the second layer, and the rest represent samples from the third layer. The sample from B2 at 19 feet is a sand lens shown in the cross sections by Creek Lands.

Table 1: Vertical Hydraulic Conductivities from Lab Testing

Borehole ID	Depth (ft)	Vertical Hydraulic Conductivity (cm/s)
B1	9	4.80E-08
	43	1.10E-07
	50	1.20E-06
B2	9	1.40E-05
	19	3.30E-03

A particle size distribution (gradation) of soils using sieve analysis on the soils was performed in accordance with ASTM D6913. This included samples from B1 at 9, 43, and 50 feet and samples from B2 at 19 feet. The samples underwent a wash that removed materials, such as clay and silt, finer than 75-µm (No. 200) sieve. The samples were then dried, weighed, and passed through sieves that ranged from 4.75 mm to 75 mm. A gradation curve was then created for each sample depending on how much soil passed the different sieves. For the sample from B2 at 9 feet ASTM D1140 was used due to it being mostly clay. The sample was washed over a 75-µm (No. 200) sieve and only a small amount of material was left remaining on the sieve. The sample was dried, weighed, and the amount of fines was noted.

For samples from B1 at 60 and 70 feet and samples at B2 at 39 and 49 feet the Caltrans Soil and Rock Logging, Classification and Presentation Manual was used (Caltrans, 2010). This manual helped identify the soil and rocks based on visual and manual procedures. Table 2 shows the soil and rock classifications based on ASTM D2478 lab tests and Caltrans Manual for visual and manual procedures. All of the samples contain clay in them and most of them are mostly clay.

Table 2: Classification of Samples from Boreholes B1 and B2 at Various Depths

Borehole	Sample Depth (ft)	Classification
B1	9	Clayey SAND w/ gravel (SC): dark gray brown, moist
	43	Sand lean CLAY (CL): olive brown, moist
	50	Clayey SAND (SC): brown, moist
	60	SANDY Lean CLAY (CL); dark gray; wet
	70	FAT CLAY with SAND (CH); dark gray; wet
B2	9	Lean CLAY (CL): dark brown, moist, some sand and gravel
	19	Clayey SAND (SC): brown, moist
	39	SEDIMENTARY ROCK (CLAYSTONE); medium grained to fine grained; olive gray; moderately to intensely weathered; very soft; very intensely fractured.
	43	SEDIMENTARY ROCK (CLAYSTONE); medium grained to fine grained; dark gray; Moderately to intensely weathered; very soft; very intensely fractured.

3.10 Layer Hydraulic Properties

The vertical hydraulic conductivities from the lab were only used from samples from B1 at 9, 43, and 50 feet. The sample from B2 at 9 feet had a very high vertical hydraulic conductivity compared to literature values based on the classification of the sample so this vertical hydraulic conductivity was ignored (USDA, 2021). The sample from B2 at 19 feet did not seem representative of the layer due to it being a small pocket of sand within the clay layer shown in Figure 13. The vertical hydraulic conductivities from the lab results seemed very low for the site and if these were representative of the whole site, it would not allow for groundwater recharge. Therefore, these values were assumed representative of the general area where samples were taken.

The porosity and specific storage were calculated from the lab results through Equations 4-5, respectively and are shown in Table 3. These porosities are within reason and the clay sample had a porosity greater than 0.3 which is reasonable for clay material.

$$n = \frac{V_v}{V_T} = \frac{V_v}{V_s + V_V} = \frac{e}{1+e} \qquad \text{(Equation 4)}$$

Where: n = porosity

V_v = volume of void-space (air and water)

V_T = total or bulk volume

V_S = volume of solids

e = void ratio

$$S_s = \gamma_w(\beta_p + n \cdot \beta_w) \qquad \text{(Equation 5)}$$

Where: S_s = specific storage (L^{-1})

γ_w = specific weight of water (Nm^{-3})

β_p = compressibility of the bulk aquifer material (m^2N^{-1})

β_w = compressibility of water (m^2N^{-1})

The compressibility of the bulk aquifer β_p depends on the type of material. For clay materials it can range from 10^{-8} to 10^{-6} and for sand it ranges from 10^{-9} to 10^{-7} (Freeze, Cherry, 1979). For the clay sample from B1 at a depth of 9 feet, a compressibility of 10^{-6} was assumed due to its clay content and for the deeper samples at 43 feet and 50 feet, a compressibility of 10^{-8} was assumed due to it being sandier.

Table 3: Porosity and Specific Storage Model Inputs from Soil Samples

Soil Sample	Porosity	Specific Storage (1/L)
B1-9'	0.35	9.81E-03
B1-43'	0.26	9.92E-05
B1-50'	0.24	9.91E-05

The hydraulic conductivities, horizontal and vertical anisotropies, specific yields, and specific storages for the three layers for the rest of the model were provided from Alex Murray's calibrated model (Murray, 2020). Layer 1 has a hydraulic conductivity that is homogenous across the site (Figure 34).

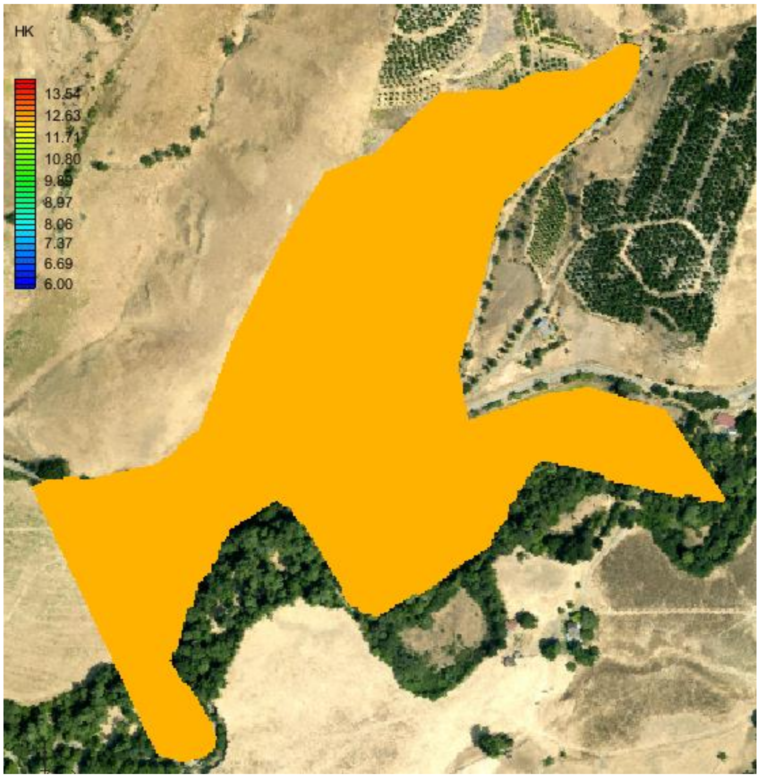

Figure 34: Layer 1 Hydraulic Conductivity (m/day)

Hydraulic conductivity for layer 2 was low for most of the site due to it being the confining layer. However, it is assumed that there is no confining layer underneath the ephemeral stream resulting in higher hydraulic conductivity. This area exaggerates the outline of the ephemeral channel and ranges in width by 10 to 20 meters (Figure 35). There is also an area of low resistivity in layer 2 from the 3D ERT survey (Figure 8), which indicates a low hydraulic conductivity (Cancroft and Carroll, 2019). This area is also where soil samples had low hydraulic conductivity.

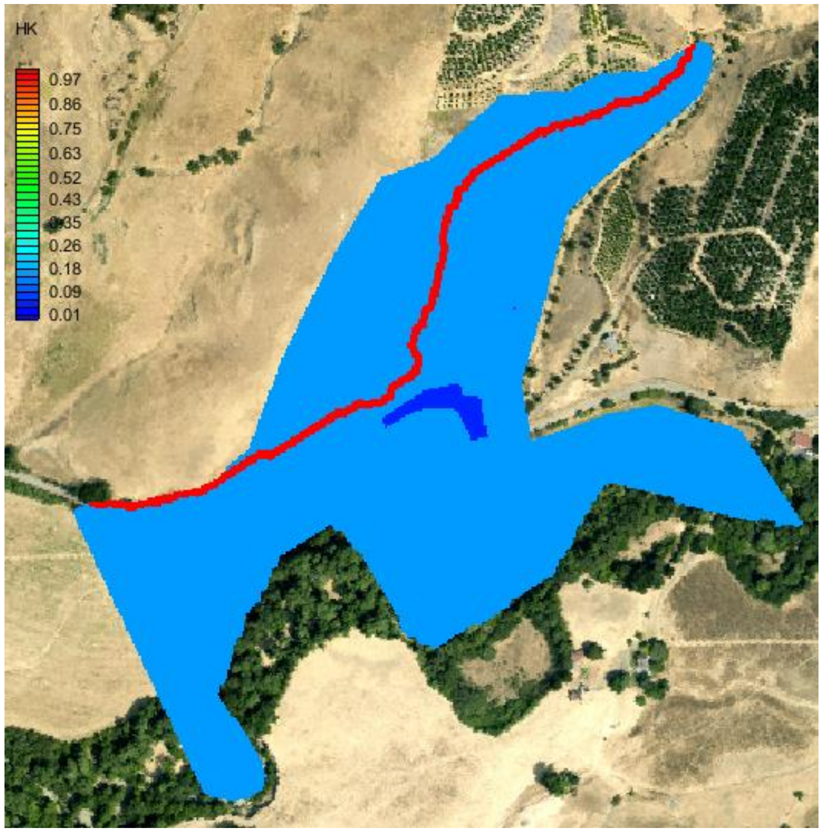

Figure 35: Layer 2 Hydraulic Conductivity (m/day). Blue, low hydraulic conductivity, to red, high hydraulic conductivity

Layer 3, the confined layer, had similar low hydraulic conductivities where the soil samples were taken and where the 3D ERT survey was performed (Figure 36). The northern portion of layer 3 has low hydraulic conductivities, but as one goes south in the model the hydraulic conductivity increases as shown in Figure 36. This alluvium runs along the Santa Rosa Creek and has a high hydraulic conductivity.

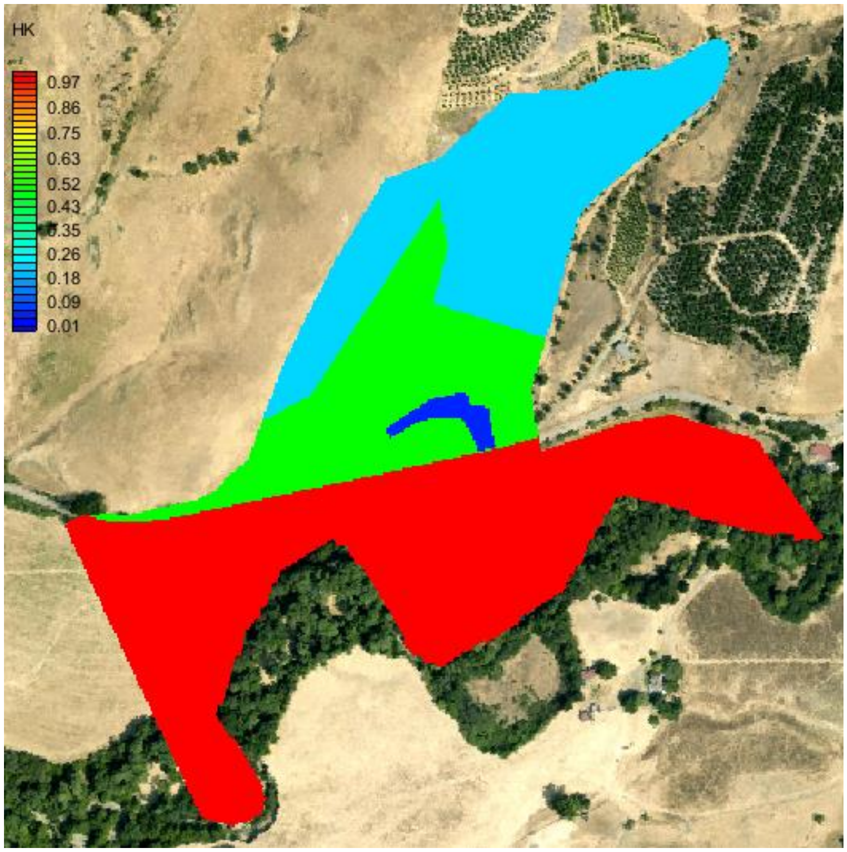

Figure 36: Layer 3 Hydraulic Conductivity (m/day). Blue, low hydraulic conductivity, to red, high hydraulic conductivity

3.11 Subsurface Barrier

Stillwater Sciences proposed subsurface barrier or "dam" that is at 65% design level and will be tied into bedrock at the Ranch to increase subsurface travel times and delay the timing of when subsurface water reaches the Santa Rosa Creek (Stillwater Sciences, 2021). The water sources for storage include precipitation, storm water runoff, and direct irrigation from the surrounding hills and the land overlying the aquifer. The groundwater is expected to travel past the proposed subsurface dam through natural leakage around the edges and an engineered pathway. There are currently two options for the engineered pathway that include either a French drain behind the dam with a pipe through the dam or a well behind the dam with a pump that will deliver stored groundwater to the creek. The subsurface barrier design is roughly 570 feet long and will be keyed into bedrock along the valley it spans. 65% design level drawings of the barrier can be seen in Appendix B of the Basis of Design Report for the Santa Rosa Creek Stream Flow Enhancement Pilot Project (Stillwater Sciences, 2021). The permeability of a subsurface barrier can range from $1.6*10^{-7}$ to $1*10^{-8}$ m/s depending on the soil-bentonite mixture used but was modeled in this study as having a permeability of $8.5*10^{-8}$ m/s, which is in the middle of the range (Ata. et. al, 2015).

CHAPTER 4. GROUNDWATER MODEL DEVELOPMENT

4.1 Background

A model is simplified representation of the complex natural world (Anderson et. al., 2015). Models can let us forecast future or past effects of the subsurface to help conceptualize hydrogeological conditions. The two types of groundwater models are physical models and mathematical models. Physical models are constructed in labs with porous material where head and flow is measured directly. Mathematical models use software that can provide analytical or numerical solutions for different equations that describe the natural world. Analytical models require a large amount of simplification in order to solve a problem mathematically and are inappropriate for most groundwater problems (Anderson et. al., 2015). Numerical models are based on the finite-difference (FD) or the finite-element (FE) method that allow for three dimensional flow through complex networks for either steady-state or transient groundwater flow. The typical workflow for a groundwater modeling process is shown in Figure 37. The basic three-dimensional groundwater flow equation that MODFLOW, a widely used groundwater flow model developed and maintained by the United States Geological Survey, solves is shown in Equation 6 (Anderson et. al., 2015).

$$\partial \frac{\partial}{\partial \mathrm{x}}\left(K_{xx}\frac{\partial \mathrm{h}}{\partial \mathrm{x}}\right) + \frac{\partial}{\partial \mathrm{y}}\left(K_{yy}\frac{\partial \mathrm{h}}{dy}\right) + \frac{\partial}{\partial \mathrm{z}}\left(K_{zz}\frac{dh}{dz}\right) = S_s\frac{\partial \mathrm{h}}{\partial \mathrm{t}} - W^* \quad \text{(Equation 6)}$$

Where: K_{xx},K_{yy}, K_{zz} = hydraulic conductivity along the x, y, and z coordinate axis that is aligned with the principal axis of the hydraulic conductivity tensor (L/T)

h = hydraulic head (L)

S_s = specific storage (L^{-1})

W = volumetric flow rate per unit volume representing sources and/or sinks of water, W<0.0 for flow out of the system, and W>0.0 for flow into the system (T^{-1})

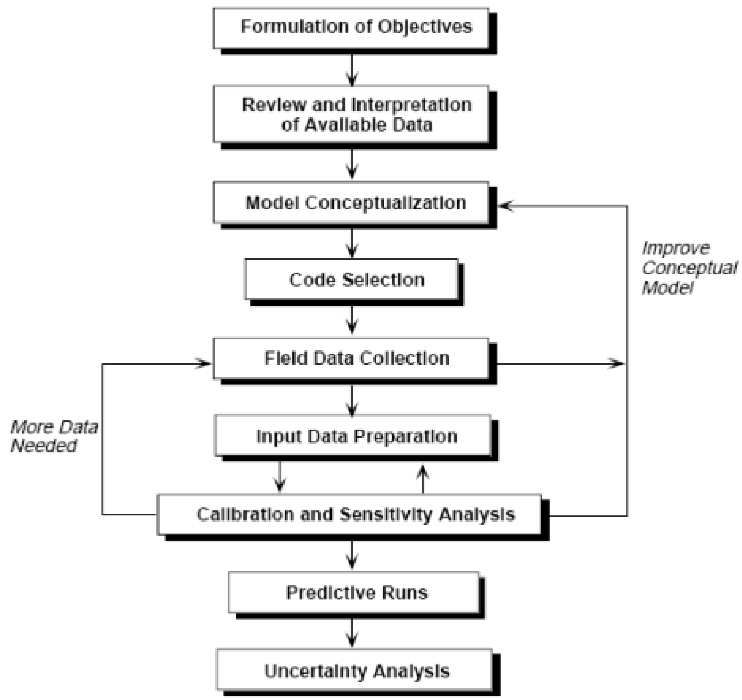

Figure 37: Workflow for Groundwater Modeling (Anderson et. al., 2015)

This study used GMS, a numerical mathematical model, to represent the groundwater at the Ranch. GMS (Groundwater Modeling System) was developed by Aquaveo, LLC to help users use a graphical user interface for various groundwater analysis. GMS has numerous programs within, but the program used for this study was MODFLOW which uses a conceptual model approach. MODFLOW is a three-dimensional, cell-centered, finite-difference, saturated flow model that can perform steady state and transient analysis. The finite-difference method MODFLOW uses in all of its cells is based on the continuity equation (Equation 7).

$$\sum Q_i = SS \frac{\Delta h}{\Delta t} \Delta V \qquad \text{(Equation 7)}$$

Where: Q_i = flow rate into cell (L^3T^{-1})

SS = specific storage (L^{-1})

ΔV = volume of the cell (L^3)

Δh = change in head over a time interval of length Δt

This study used transient data at different time steps, such as boundary conditions, streamflow, pumping, recharge, and evapotranspiration rates. MODFLOW defines time steps using the term stress periods. Stress periods are created when there is a change in a stressor (e.g., pumping, recharge, etc.).

The design of a groundwater model should consider data such as geomorphology, geology, geophysics, climate, vegetation, soils, hydrology, hydrochemistry/geochemistry, and anthropogenic aspects (Anderson et. al., 2015). These components need to be refined through an iterative process through trial and error and calibration to model the real-world groundwater condition. Measured data can include observed head, base flow, spring flow, infiltration from a losing stream, groundwater inflow to a lake, and evapotranspiration across the water table.

4.2 Setup

4.2.1 Previous Model

The previous model was set up by Alex Murray, a Civil/Environmental Graduate Student in 2020 (Murray, 2020). Murray started the modeling process by processing geospatial data in ArcMap and then importing it into GMS to create the groundwater model of the Ranch.

In ArcMap a 2m, raster and shapefiles were clipped to form the extents of the model. The projection for the model was set to Albers Conic Equal Area Zone, NAD83 in meters. The shapefiles were then converted into coverages for GMS. The coverages modeled the data described in Chapter 3 such as the extent of the model, variable head boundaries, streams, agricultural well, recharge, evapotranspiration rates, observation wells, and hydraulic properties on the three layers. In MODFLOW the model was set to transient to run the transient data, and the MODFLOW version was Newton (NWT). NWT version uses the Upstream Weighting (UPW) package to allow the wetting and drying of cells to help with convergence. Optional packages were added to the model such as Time-Variant Specified Head (CHD), Evapotranspiration (EVT), Multi-Node Well (MNW1), Parameter Estimation with Advanced Spatial Parameterization (PEST-ASP), Recharge (RCH), and Stream (STR). The previous model was calibrated to data from 2016-2017. The previous model by Murray had nine estimated parameters for the model calibration. These included hydraulic conductivities and horizontal anisotropies for layer 1, layer 2, layer 2 under the ephemeral channel as well as northern area of layer 3, and southern area of layer 3, in addition to the stream conductance for the ephemeral channel. The results of the model fairly represented the groundwater heads observed. The distribution of observed vs simulated heads from Murray's model is shown in Figure 38.

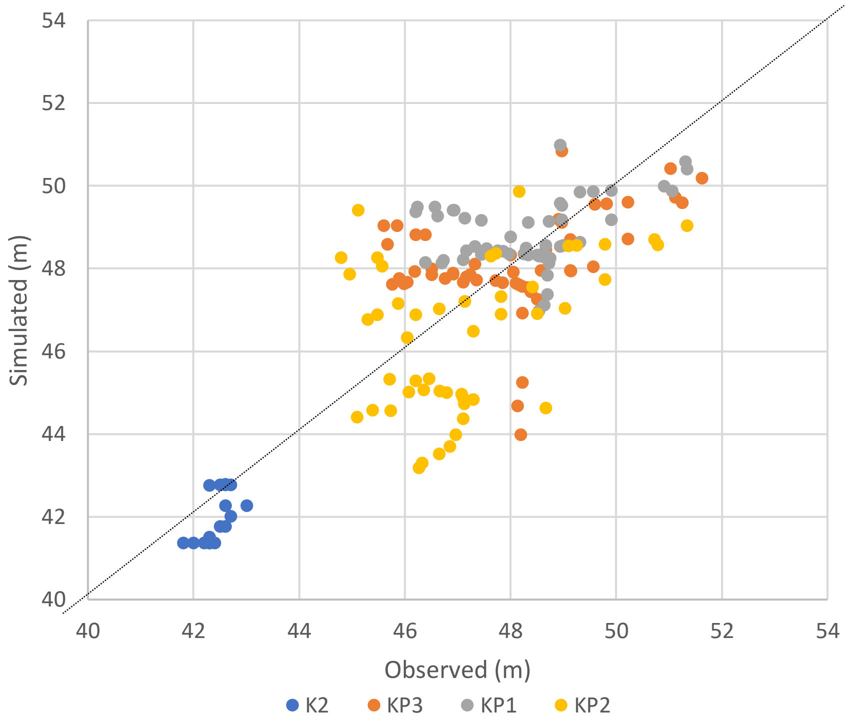

Figure 38: Observed vs Simulated Heads from Alex Murray's Model.

4.2.2 Updated Model

The updated model includes recommended adjustments from Alex Murray and Dr. Muleta, as well as new data. One of the first adjustments included changing all of the daily data to monthly data. This sped up the model runtime and calibration times significantly. Another adjustment made to the model included redefining the elevations of the second and third layer from the cross sections drawn by Creek Lands Conservation. This was done manually by manipulating elevations in the cells for the two layers (Figure 39).

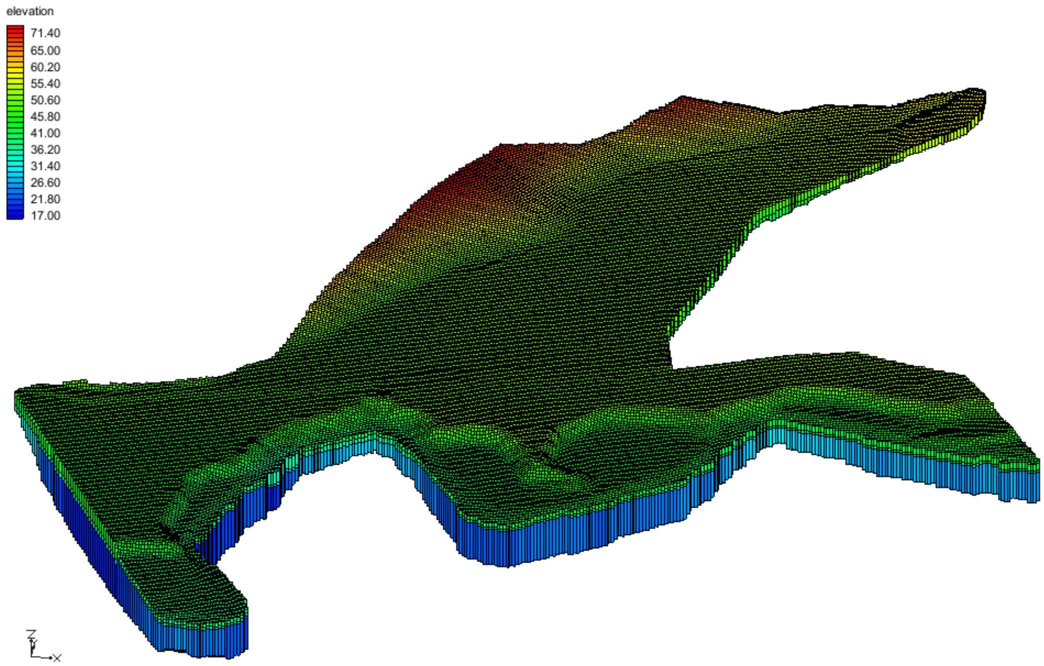

Figure 39: 3D GMS MODFLOW Model Showing Elevations of the Model in Meters.

The lab data gave information regarding vertical hydraulic conductivity, porosity, and specific storage for parameter inputs. This information was only used in the areas where soil samples were taken (Figure 35-Figure 36), due to the vertical hydraulic conductivities from the lab seeming low for the overall site. The previous model only had inputs for the horizontal hydraulic conductivity, while this model includes vertical hydraulic conductivity inputs. The horizontal hydraulic conductivity in the areas where samples were taken was assumed to be 100 times larger than the vertical hydraulic conductivity (Table 4). This 100:1 ratio is typical for clay (Yeh, 2018). The third layer had two tested samples. A weighted average of the vertical hydraulic conductivities of the two samples was used based on the depths of the clayey sand and the sandy lean clay in layer 3 (Figure 12).

Table 4: Model Inputs for Tested Samples

Parameter	Horizontal Hydraulic Conductivity (m/d)	Vertical Hydraulic Conductivity (m/d)
Layer 2	4.15E-03	4.15E-05
Layer 3	3.87E-02	3.87E-04

Another addition to the model included adding mountain front recharge and adjusting pumping rates based on new data discussed in Section 3.4 and 3.5.3. The horizontal flow barrier (HFB) package within MODFLOW was used to model the subsurface barrier. The proposed subsurface barrier was modeled with a hydraulic conductivity of $7.34*10^{-3}$ m/d, 174 meters in length, 1 cell width (2 meters) wide, and the depth going to bedrock, bottom of layer 3 (Figure 40).

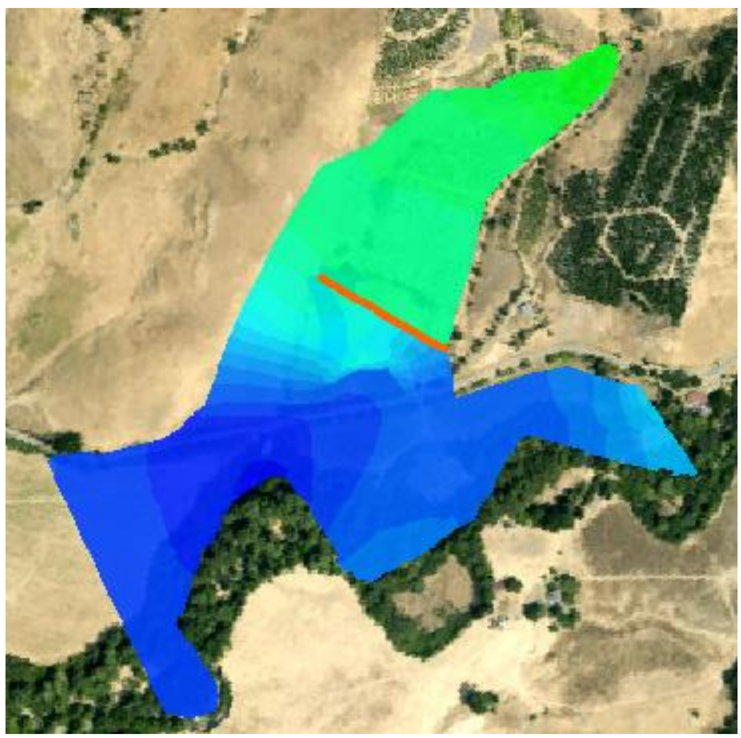

Figure 40: Proposed Subsurface Barrier in Orange Modeled in GMS

Once all of the additional new coverages were mapped and data were entered into MODFLOW, the model was run. With the addition of all the new adjustments to the model the next step was to calibrate it to make the simulated heads in the model match the observations.

4.2.3 Calibration

Once the model with data from 2015 to 2019 was able to run without errors the built-in package in MODFLOW known as PEST-ASP was used to calibrate the model. PEST-ASP is an automated parameter estimation that determines optimal (i.e., best fit) parameter values from observations through statistical formulas so the user doesn't have to manually do trial and error to obtain parameters to better represent the model to real-world observations (Aquaveo, 2019). The parameter estimation can calibrate hydraulic conductivities, anisotropy, storage coefficients, recharge, and stream conductance. This study calibrated hydraulic conductivities, horizontal anisotropy, and stream conductance, in total 15 parameters. The goal of the calibration is to reduce the difference between simulated values and observed values by decreasing or increasing the contribution of individual residuals to the total sum of model error called the objective function, Φ (Anderson et. al., 2015). The PEST objective function is based on the sum of squared differences shown in Equation 8. By minimizing the phi value the differences in simulated and observed data decrease.

$$\Phi = \{\sum_{i=1}^{n}[w_{\mathrm{h}i}(\mathrm{h}_m - \mathrm{h}_s)_i]^2 + \sum_{i=1}^{n}[w_{\mathrm{f}i}(\mathrm{f}_m - \mathrm{f}_s)_i]^2\} \qquad \text{(Equation 8)}$$

Where: Φ = phi objective function

w_{hi} = weight for the ith head observation

h_m = measured (observed) head target

h_s = simulated equivalent head

w_{fi} = weight for the ith flux observation

f_m = measured (observed) flux target

f_s = simulated equivalent flux

The data in this model included water level measurements from 2015 to 2019 for calibration compared to the previous model, which used data from 2016 to 2017. The number of stress periods decreased from 731 stress periods in the previous model calibration to 60 stress periods in this study due to the monthly time steps. This model had 15 parameters for the model calibration shown in Table 5. The initial values for the nine estimated parameters in the model were set to values that converged on the initial run in Murray's model. The other initial values were based on literature values (USDA, 2021). The observation data that the model was calibrated to is limited to only four wells, three of which are in close proximity. The lack of observations throughout the site means that water elevations in other parts of the site cannot be verified.

Table 5: Initial Values for Soil Properties for PEST

Parameter	**Value**
Hydraulic Conductivity of Layer 1	12.6 m/d
Horizontal Anisotropy of Layer 1	1.0
Hydraulic Conductivity of Layer 2	0.1 m/d
Horizontal Anisotropy of Layer 2	1.0
Hydraulic Conductivity of Layer 2 under the ephemeral channel	0.5 m/d
Horizontal Anisotropy of Layer 2 under the ephemeral channel	1.0
Horizontal Anisotropy of Soil Sample in Layer 2	1.0
Horizontal Anisotropy of Soil Sample in Layer 3	1.0
Hydraulic Conductivity of Northern Layer 3	0.2 m/d
Horizontal Anisotropy of Northern Layer 3	1.0
Hydraulic Conductivity of Layer 3 near Wells	0.5 m/d
Horizontal Anisotropy of Layer 3 near Wells	1.0
Hydraulic Conductivity of Southern Layer 3	50.0 m/d
Horizontal Anisotropy of Southern Layer 3	1.0
Stream Conductance of Ephemeral Stream	0.0296 (m^2/d)/m

The calibration was an iterative process to find the right parameters by adjusting different zones of hydraulic conductivity and data to have the model not overestimate or underestimate the observed head. During the calibration, the Φ values dropped by 30% in over 50 iterations. The “optimal” parameter values from PEST are shown in Table 6. These values are optimal due to PEST not being able to decrease the difference between simulated and observed head. PEST predicted reasonable parameters for each layer and zone based on the simulated heads compared to observed heads.

Table 6: Parameters from PEST

Parameter	**Value**
Hydraulic Conductivity of Layer 1	14.79 m/d
Horizontal Anisotropy of Layer 1	1.0
Hydraulic Conductivity of Layer 2	0.17 m/d
Horizontal Anisotropy of Layer 2	1.0
Hydraulic Conductivity of Layer 2 under the ephemeral channel	1.0 m/d
Horizontal Anisotropy of Layer 2 under the ephemeral channel	1.0
Horizontal Anisotropy of Soil Sample in Layer 2	0.2
Horizontal Anisotropy of Soil Sample in Layer 3	0.2
Hydraulic Conductivity of Northern Layer 3	0.21 m/d
Horizontal Anisotropy of Northern Layer 3	1.0
Hydraulic Conductivity of Layer 3 near Wells	0.51 m/d
Horizontal Anisotropy of Layer 3 near Wells	1.0
Hydraulic Conductivity of Southern Layer 3	49.98 m/d
Horizontal Anisotropy of Southern Layer 3	1.0
Stream Conductance of Ephemeral Stream	0.0366 $(m^2/d)/m$

A comparison of the observed and simulated head for the four observation wells is given in Figure 42. Overall, the model tends to overestimate the heads at wells KP1, KP2, and KP3, but seems to capture the trend reasonably well. Figure 42-Figure 45 show the time series plots of the simulated and observed heads for all four wells.

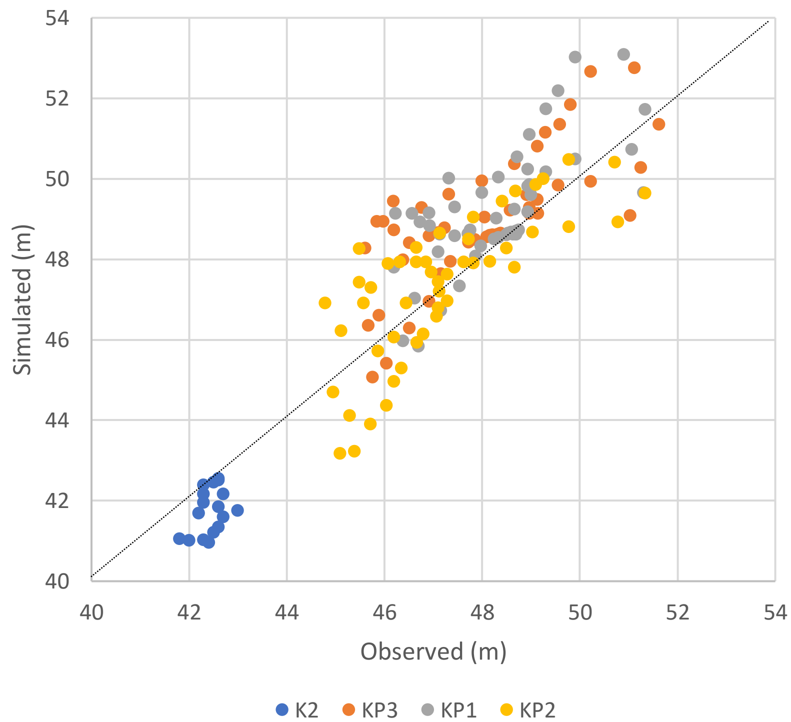

Figure 41: Observed vs Simulated Head for Calibrated Model

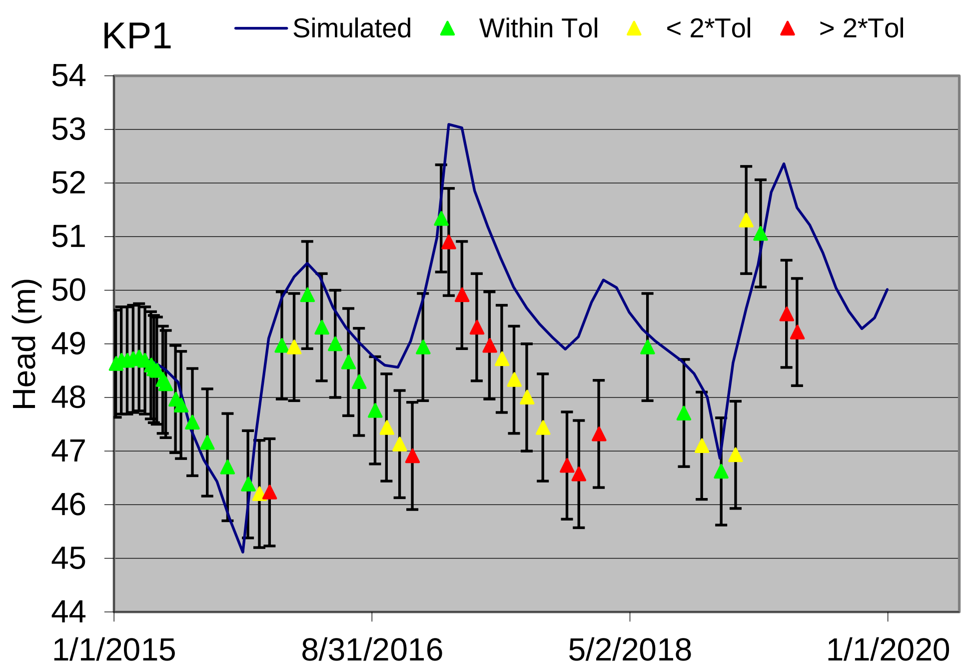

Figure 42: Observed Head Values (triangles) at Well KP1 Compared to Calibrated Model Simulated Heads with 1m Tolerance

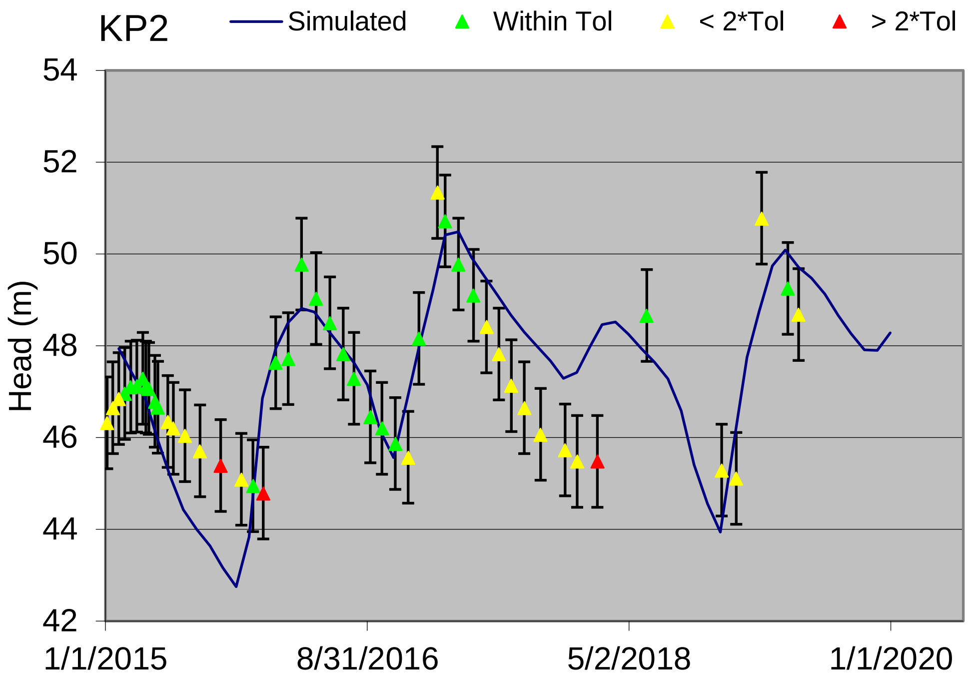

Figure 43: Observed Head Values (triangles) at Well KP2 Compared to Calibrated Model Simulated Heads with 1m Tolerance

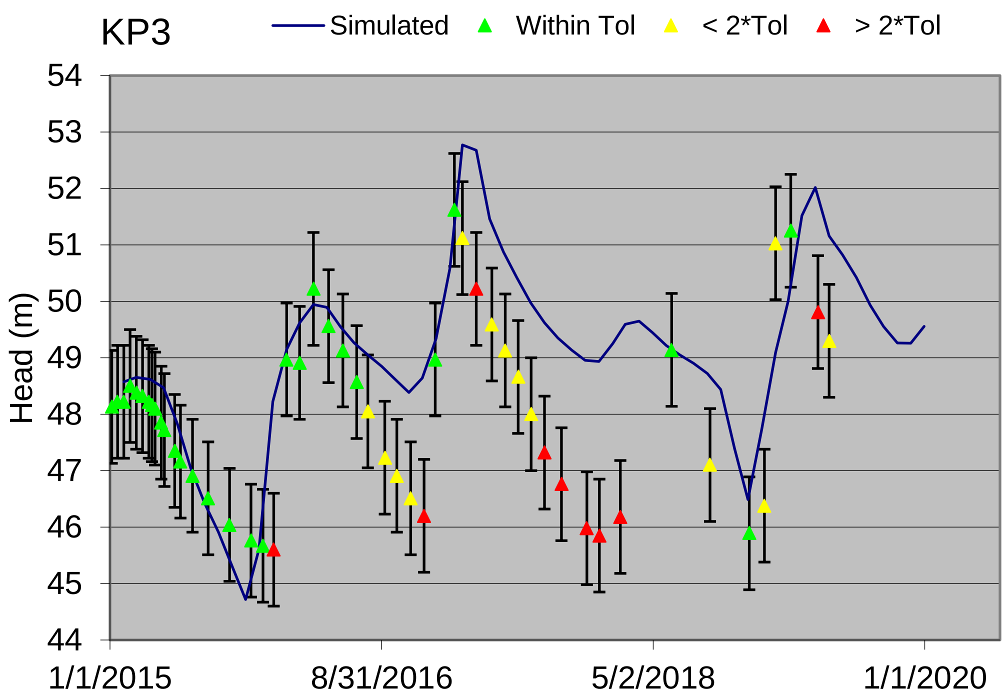

Figure 44: Observed Head Values (triangles) at Well KP3 Compared to Calibrated Model Simulated Heads with 1m Tolerance

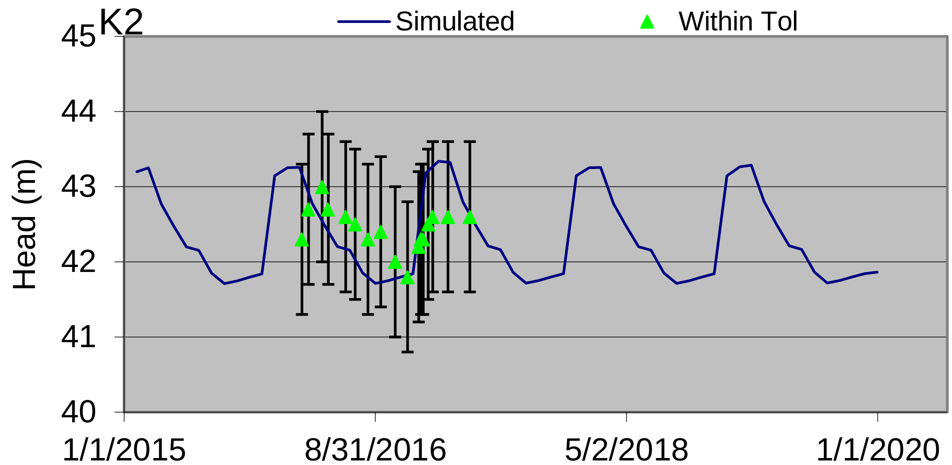

Figure 45: Observed Head Values (triangles) at Well K2 Compared to Calibrated Model Simulated Heads with 1m Tolerance

Goodness of the calibration effort can be evaluated using quantitative measures such as root mean square error (*RMSE*), correlation coefficient (*R*), and the coefficient of determination (R^2) to determine the accuracy. The RMSE indicates a perfect relationship between observed and predicted values when it is equal to 0 and as it increases the relationship gets worse. The correlation coefficient, R, is also a tool to assess the strength of the relationship between the observed and measured, where 0 is a poor relationship and 1 is a strong relationship. The last statistical method used was R^2, which measures how close the data is related to each other, 1 being a perfect fit. Table 7 shows that through the additional information and adjustments to the site, as well as calibration, the model has improved, and the simulations can be considered “Very Good” based on performance evaluation criteria for hydrologic models such as the R^2 being greater than 0.80 (Moriasi, 2015).

Table 7: Statistical Analysis of Previous Model to Current Model

Model	RMSE	R	R^2
Previous Model (2020)	0.004938	0.76	0.58
Current Model (2021)	0.002967	0.90	0.81

CHAPTER 5. RESULTS & DISCUSSION

This chapter discusses the results of the calibrated model at the Ranch. The model allows for evaluation of the hydraulic properties of the soil, the existing recharge basin, and the proposed subsurface barrier. From 2015 to 2019 the Ranch experienced the lowest ground water levels in November of 2015, (Figure 46a) and experienced the highest groundwater levels in March of 2017 (Figure 46b). These high- and low-level groundwater shows there is a large change in head levels at the Ranch, especially in the northern area of the site.

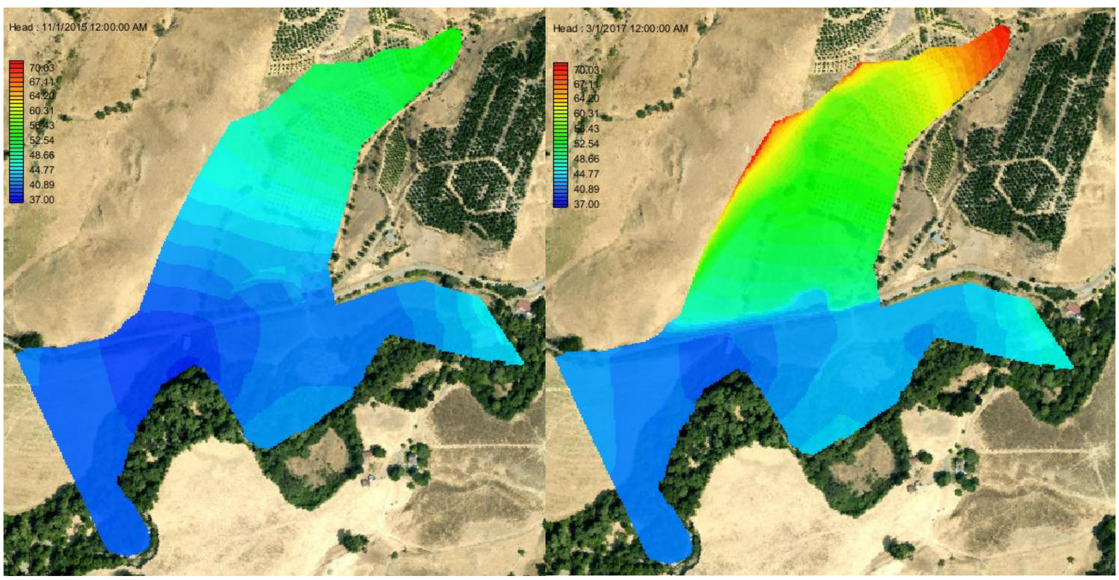

(a) (b)

Figure 46: Lowest (a) and Highest (b) Groundwater Levels within the Ranch (Blue Showing Low levels and Red Showing High Levels) (Head in Meters)

5.1 Parameters

The calibrated parameters are shown in Table 6. These values can give us more insight to the subsurface and aquifer characteristics. Overall, the calibrated hydraulic properties do confirm that there is a topmost layer with suitable infiltration over a clay confining aquifer. The northern part of the site in the third layer is comprised of a low hydraulic conductivity soil that is similar to the confining clay layer. Therefore, artificial recharge will not be effective in the northern area of the Ranch. In the southern part of the site, recharging is possible due to the alluvium in layer three. However, this is close to Santa Rosa Creek and the recharged water could enter the creek quickly (before summer).

The results from the soil samples in terms of hydraulic conductivity are significantly different from the calibrated parameters in the model. This could be due to a large variability of soils throughout the project area.

5.2 Flow Duration and Travel Times

During a typical year, the groundwater flows from the northern area of the site to the southern area of the site and only reaching the third layer confined layer near the southern portion of the site. Most of the vertical travel time of the water is in the second confining layer. Figure 47 shows the movement of water from the northern area of the site to the southern part. Groundwater flows out into the Santa Rosa Creek and the southwest boundary of the site. This trend is generally the same through the years for each month.

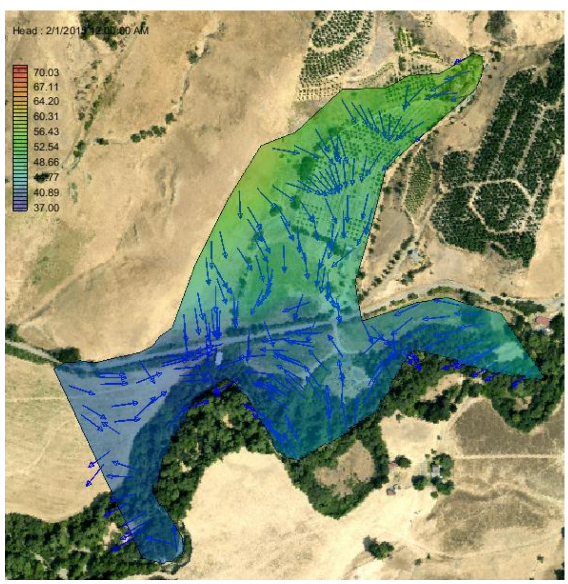

Figure 47: Groundwater Flows Directions for a Typical Month (Head in Meters)

5.2.1 Existing Recharge Basin

The water from the recharge basin spends quite a bit of time in the second confining layer due to the low hydraulic conductivity. A flow path analysis of the water from the recharge basin was performed using the MODPATH extension within GMS. The first flow path analysis that was performed was for a duration of one year, from 2015-2016 (Figure 48). The water only flowed roughly 50 meters and stayed in confining second layer (Figure 49).

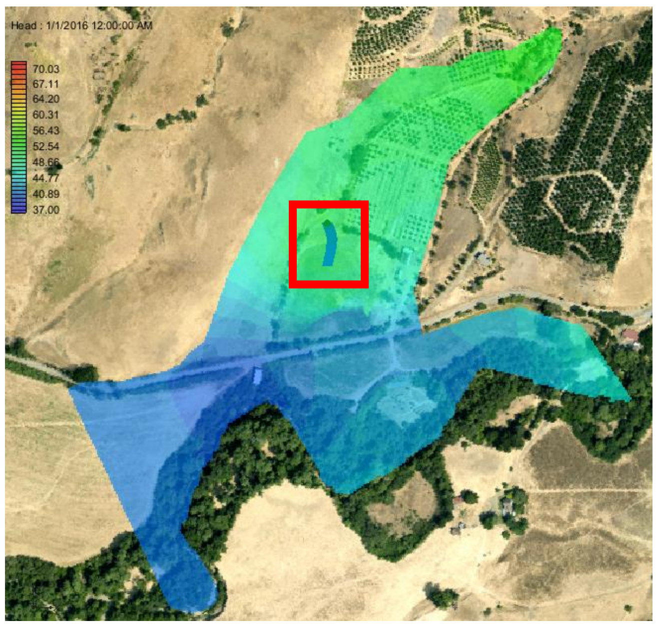

Figure 48: One-Year Flow Duration Length of Water from Existing Recharge Basin (Head in Meters)

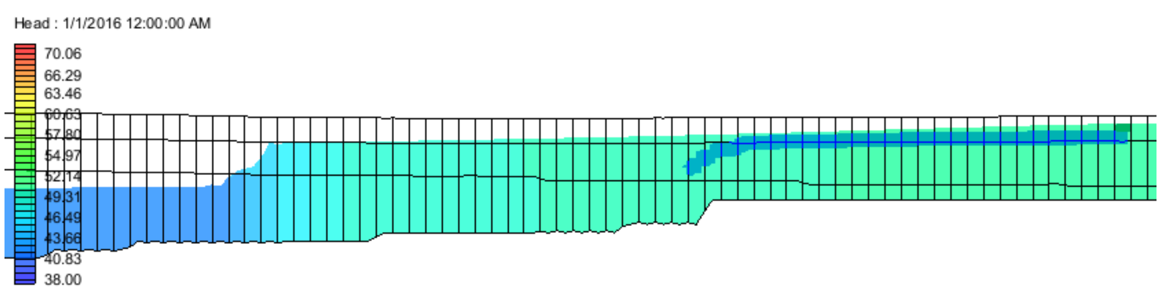

Figure 49: Cross-Section of One-Year Flow Duration Length of Water from Existing Recharge Basin (Head in Meters)

An analysis of the two-year flow path, 2015-2016, was done and it had a total length of 75 meters. It can be seen that water starts to flow into the confined layer at the end of the time period (Figure 50). Groundwater has to flow through the second confining layer to get to the creek due to water levels being low at certain times of the year. This is before the third layer becomes alluvium in the southern area of the site.

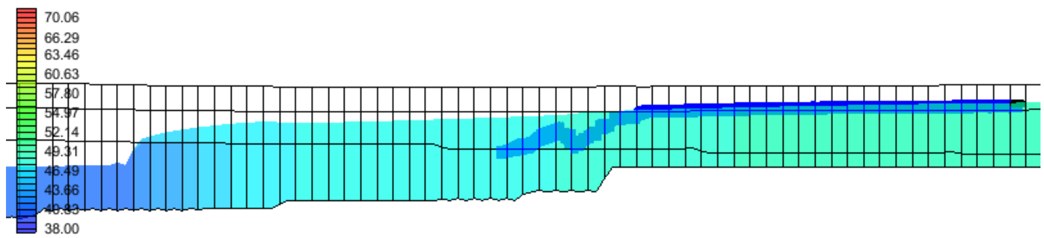

Figure 50: Cross-Section of Two-Year Flow Duration Length of Water from Existing Recharge Basin Flowing into Confined Layer (Head in Meters)

During a three-year MODPATH analysis, the water can be seen extending closer to the creek as it moves in layer 3. (Figure 51).

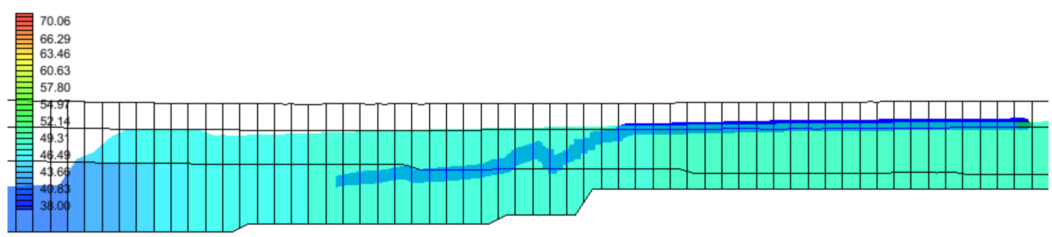

Figure 51: Cross-Section of Three-Year Flow Duration Length of Water from Existing Recharge Basin Flowing into Confined Layer (Head in Meters)

For a four-year flow path analysis the water still hasn't gone into the alluvium of the third layer and is still approaching the creek (Figure 52).

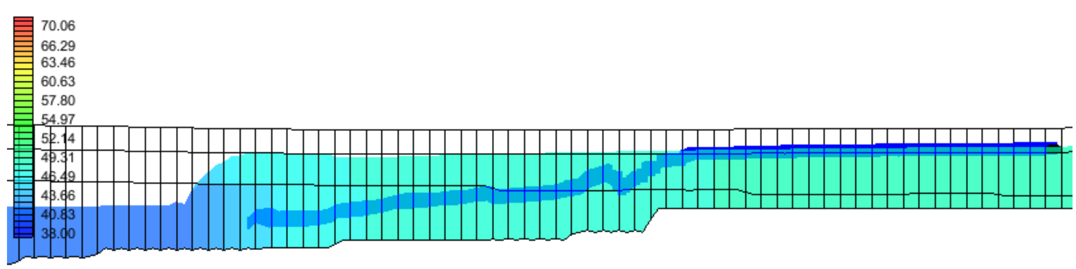

Figure 52: Cross-Section of Four-Year Flow Duration Length of Water from Existing Recharge Basin Flowing into Confined Layer (Head in Meters)

The last flow path analysis of the existing recharge basin included the total five-year duration of the model. During this time period the groundwater from the recharge basin flowed into the alluvium in layer 3. This sped up the flow of groundwater due to the high hydraulic conductivity. The flow path extends all the way to Santa Rosa Creek where it outfalls (Figure 53-Figure 54).

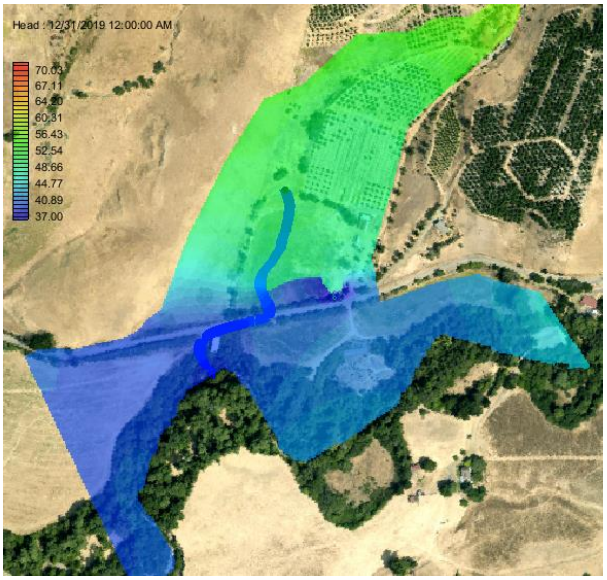

Figure 53: Five-Year Flow Duration Length of Water from Existing Recharge Basin (Head in Meters)

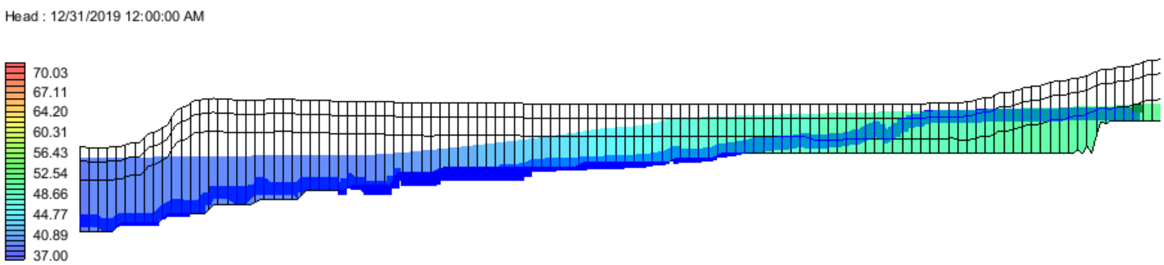

Figure 54: Cross-Section of Five-Year Flow Duration of Water from Existing Recharge Basin Flowing into Confined Layer Shown in Dark Blue (Head in Meters)

It can be concluded that the recharge basin does help recharge the confined aquifer over a long term, such as two years. This disputes the findings done in the previous model that peroration of groundwater into the confined aquifer wasn't possible.

The clay confining layer slows down the movement of flow through it, but water does eventually percolate into the underlying aquifer and after five years outfalls to the creek.

5.2.2 Subsurface Barrier

The proposed subsurface barrier "dam" that was modeled increased travel times and delayed the timing of the groundwater flows to Santa Rosa Creek. The figures below show the comparison of the effects the subsurface barrier has on groundwater levels for the same time period (Figure 55). Throughout the year the subsurface barrier holds the water back and keeps it longer in the northern area of the site. This could allow for percolation of water through the confining layer.

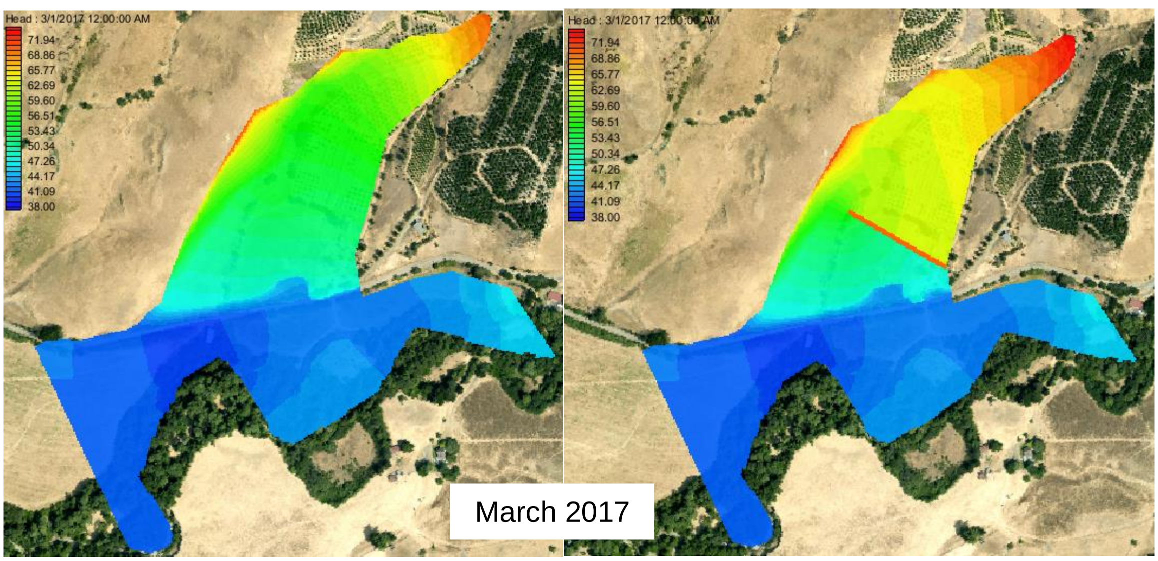

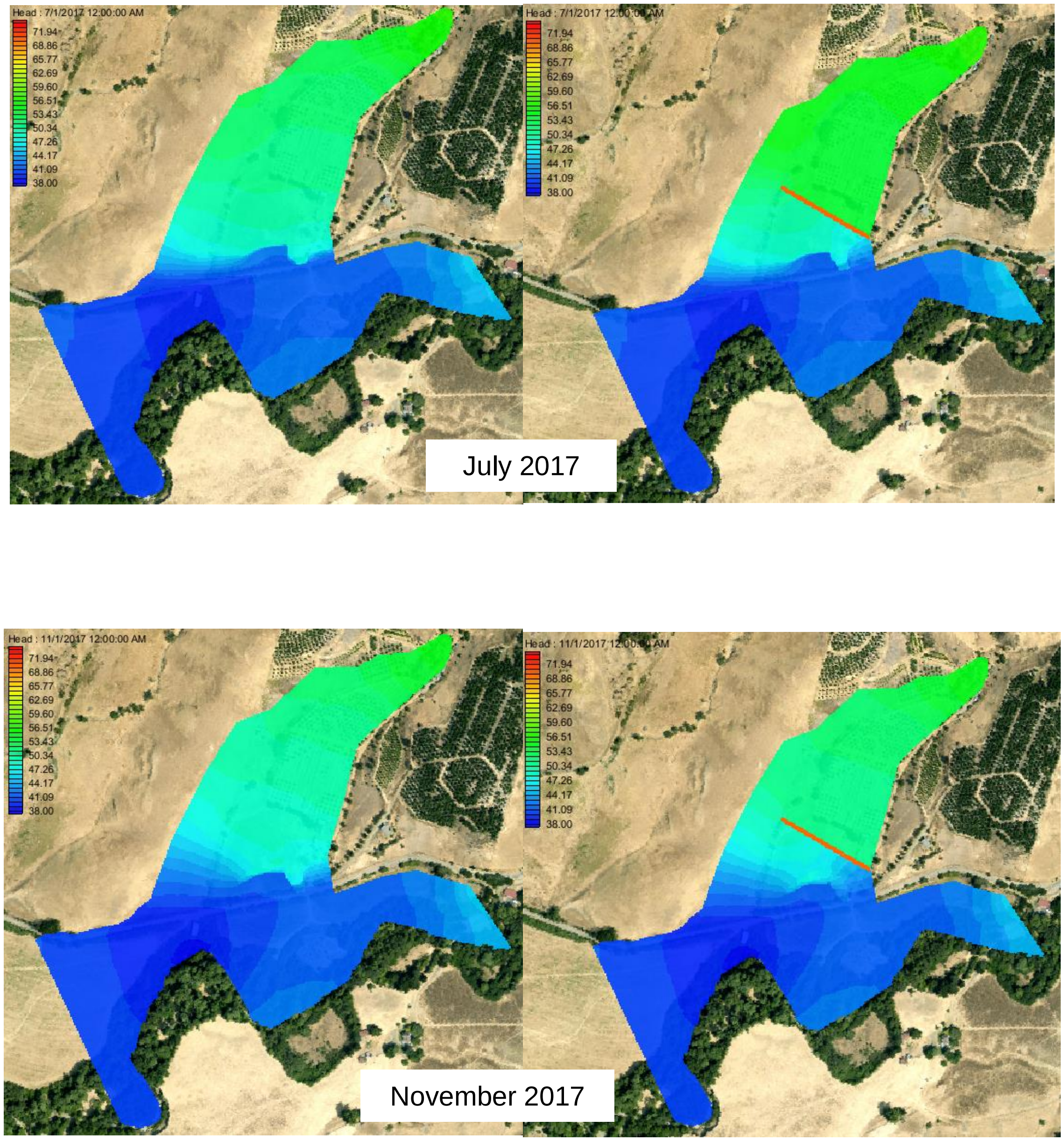

Figure 55: Comparison of Heads (m) from March, July, and November from Subsurface Barrier

Another MODPATH analysis was done for the existing recharge basin with the subsurface barrier. The analysis was done over the five-year period. It can be seen in Figure 56 that the barrier slows down the flow from the recharge basin. Figure 57 shows that the barrier allows water to percolate into the third confined layer.

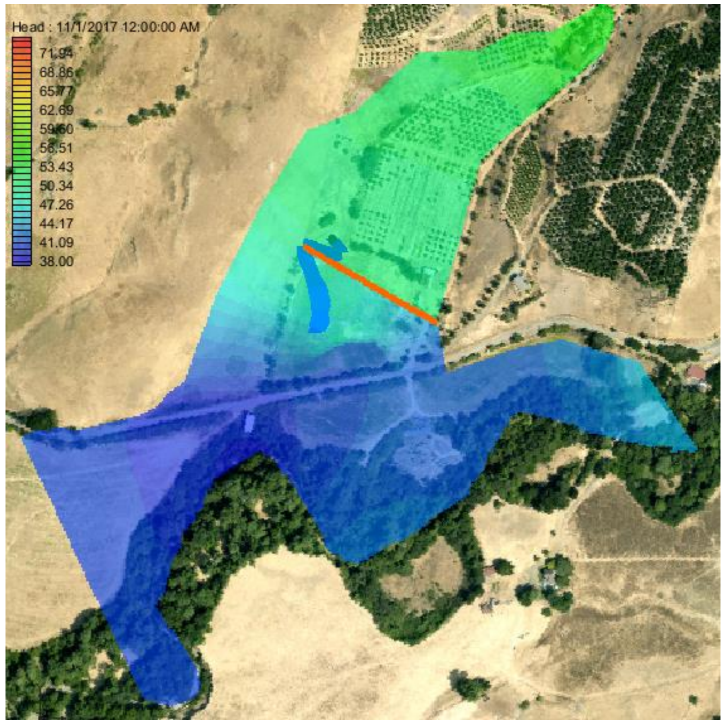

Figure 56: MODPATH Analysis of Existing Recharge Basin with Subsurface Barrier

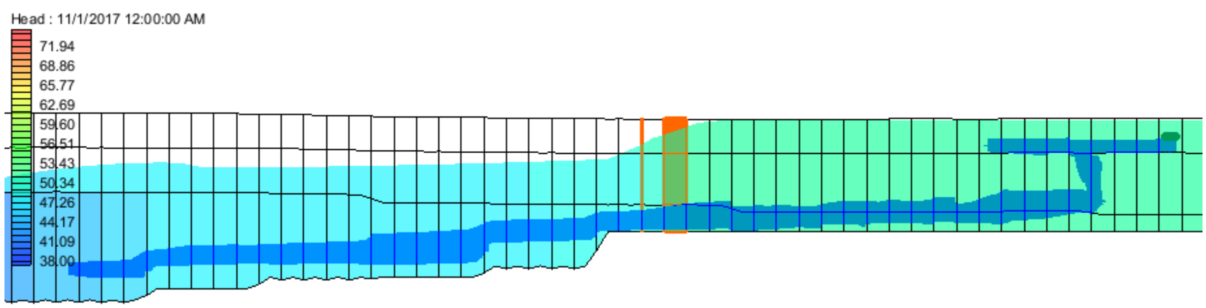

Figure 57: Cross-Section of Five-Year Flow Duration of Water (Shown in Dark Blue) from Existing Recharge Basin Flowing into Confined Layer being Delayed by the Subsurface Barrier

A comparison was done of travel times of water from the existing recharge basin during existing conditions and with the proposed subsurface barrier. It was seen that the subsurface barrier allowed for percolation of water into the underlying groundwater aquifer only after 321 days. The existing conditions don't allow for percolation of water until 715 days after water infiltrates from the recharge basin (Table 8).

Table 8: Travel Times of Water from Existing Recharge Basin into Layers 1, 2, and 3 with Existing Conditions and Proposed Subsurface Barrier

Travel Times of Water into Layers with Existing Conditions (Days)			Travel Times of Water into Layers with Subsurface Proposed Barrier (Days)		
Layer 1	Layer 2	Layer 3	Layer 1	Layer 2	Layer 3
0	78	715	0	52	321

A mass balance of each layer was done for each of the 5 years of data for the existing conditions and for the proposed barrier. The top layer stayed the same for both conditions since it is just reliant on the recharge from the surface. Layer 2 had minimal volume within it since it is a thinner layer compared to layer 1 and layer 3. Layer 3, the confined aquifer, overall increased the volume of water each year compared to the existing conditions. During drought years, such as years 2016-2017 and 2019-2020, the volume of water held only increased by roughly 1,700 m^3 and 1,500 m^3 respectively. During 2017-2018 and 2018-2019, fairly wet years, the water held within the aquifer increased by 7,000 m^3 and 8,500 m^3 respectively (Table 9).

Table 9: Volume of Water in Each Layer from Recharge with Existing Conditions and with the Proposed Subsurface Barrier

	Existing Conditions Volume (m^3)			Proposed Subsurface Barrier Volume (m^3)			Increase in Volume In Confined Aquifer (m^3)
Year	Layer 1	Layer 2	Layer 3	Layer 1	Layer 2	Layer 3	
2015-2016	21,527	4,466	43,237	21,527	3,147	50,644	**7,407**
2016-2017	105,751	4,124	53,700	105,751	5,125	55,379	**1,679**
2017-2018	12,134	1,987	38,455	12,134	1,899	45,457	**7,002**
2018-2019	18,063	3,495	40,410	18,063	2,317	48,979	**8,569**
2019-2020	48,996	1,183	5,979	48,996	2,145	7,501	**1,522**

CHAPTER 6. CONCLUSION AND RECOMMENDATIONS

6.1 Conclusion

The objective of this modeling effort was to test if the existing recharge basin could recharge the confined aquifer and to analyze the effects of a subsurface barrier. Refinement of a previous model and through integration of more detailed information helped to improve the general understanding of the recharge characteristics of the Ranch aquifer system. This study has successfully improved the accuracy of the groundwater model previously developed for the Ranch. Based on reported model-data fitting metrics, RMSE, R, and R2, the model simulations are very good when compared to observations. A major conclusion of this study is that recharging the groundwater basin does augment the confined aquifer. This takes two years to seep into the confined aquifer and during some years the volume of water in the confined aquifer is up to 53,000 m^3. The recharge basin also infiltrates into the Santa Rosa Creek after a five-year time period. This result refutes findings of the previous model that the low conductivity soil in the northern portion of layer 3 prevents water from percolating deeper. The proposed subsurface barrier can also delay travel times of the groundwater and will enhance recharge to the confined aquifer on average of 5,200m^3 per year. This will happen farther north on the Ranch, where the subsurface barrier is located, rather than farther south on the Ranch. Overall, in the existing conditions it still takes up to five years for groundwater to travel to the creek, so the barrier wouldn't help substantially in slowing water to the creek overall, but does increase the volume of water into the confined aquifer by a faster time period.

Overall, this study showed that artificial recharge is feasible for the Ranch and the subsurface barrier could be effective. Although soil samples tested were not representative of subsurface condition of the entire site, they were helpful for the model improvement.

6.2 Future Recommendations

6.2.1 Modeling

The groundwater model could be improved by expanding the model in the northern area of the site to analyze the effects of a new proposed basin by Stillwater Sciences. This can help to see if artificial recharge can occur in the northern area of the site. The subsurface barrier should be modeled with the engineered pathways when the 100% design phase is completed. These engineered pathways recommended from Stillwater Sciences include either a French drain behind the barrier with a pipe going through the dam or a pump that would deliver stored groundwater to the creek. A pump would be easiest to design in GMS since it will be only pumping at specific times of the year and that can be specified within MODFLOW.

Another modeling recommendation would be to parametrize the vertical anisotropy. This would add another eight parameters to calibrate and will increase the calibration time. For calibration of the model a calibration tool called Pilot Points can be used to help. Instead of the zonal approach calibration done in this study, a pilot approach creates points spaced evenly throughout the site to allow values of hydraulic conductivity to range more within a layer. The zonal approach, for calibration, did not capture the full heterogeneity of the hydraulic conductivity within the model.

6.2.2 Data Needs

Additional borehole explorations across the site could provide a better understanding of the subsurface. These boreholes should be more evenly placed across the Ranch, such as the western and northern parts, and the depths should go to bedrock. Along with the boreholes, soils samples should be tested to analyze the hydraulic properties. The past data exploration test samples weren’t as helpful as expected due to it having samples of very low hydraulic conductivity which doesn’t represent the overall site.

The agricultural well observation data should be up to date to get a better understanding of groundwater levels in the southern portion of the site near Santa Rosa Creek. The groundwater levels from the piezometers that were added to the site in 2020 should be added to the model once they are finalized. This will give the model more observations to calibrate too. More observation wells should be added to the site so there can be more data to help calibrate the model. The placement of them should be in the northern, western, and southern portions of the site, since there are concentrated in the eastern portion of the site. The three existing wells are too close in proximity to say that the whole model is similar to these areas. A monitoring plan should be put in place as well to make sure data is retrieved at least every month.

REFERENCES

Anderson, M.P., Woessner W.W., Hunt, R.J., (2015). *Applied Groundwater Modeling. Simulation of Flow and Advection Transport*.

Aquaveo, LLC. (2019). *GMS User Manual 10.4*. Retrieved from GMS Wiki: https://www.xmswiki.com/wiki/GMS:GMS_User_Manual_10.4

ASTM International. (2016). *ASTM D 5084-16a: Standard Test Methods for Measurement of Hydraulic Conductivity of Saturated Porous Materials Using a Flexible Wall Permeameter.*

ASTM International. (2017a). *ASTM D 1140-17: Standard Test Methods for Determining the Amount of Material Finer than 75-µm (No. 200) Sieve in Soils by Washing.*

ASTM International. (2017b). *ASTM D 2487-17: Standard Practice for Classification of Soils for Engineering Purposes (Unified Soil Classification System).*

ASTM International. (2017c). *ASTM D 6913-17: Standard Test Methods for Particle-Size Distribution (Gradation) of Soils Using Sieve Analysis.*

Ata, A.A., Salem, N. T., Elkhawas, M. N. (2015). *Properties of soil–bentonite–cement bypass mixture for cutoff walls.* Retrieved from https://www.sciencedirect.com/science/article/pii/S0950061815005619

Bouwer, H., & Rice, R. C. (1989). *Effect of Water Depth in Groundwater Recharge Basins on Infiltration*. Journal of Irrigation and Drainage Engineering, 556-567.

Bouwer, H. (1999). *Artificial recharge of groundwater: Systems, design, and management*, Ch. 24. In L. Mays, Hydraulic Design Handbook. New York: McGraw-Hill.

Cal Poly SLO. (2020). *California Evapotranspiration Data*. Retrieved from Irrigation Training & Research Center: http://www.itrc.org/etdata/index.html

Caltrans. (2010). *Soil and Rock Logging, Classification, and Presentation Manual 2010 Editon.*

Cancroft, O., and Carrol, A. (2019) *Geophysical Analysis of Kendall Ranch and Santa Rosa Creek.*

Cleath, T. S. (2019). *Hydrogeologic Characterization Middle Reach Santa Rosa Creek Valley Alluvium: Santa Rosa Creek Flow Enhancement Pilot Project.* San Luis Obispo: Cleath-Harris Geologists, Inc.

Creek Lands Conservation. (2020). Cross-Sections Created from Dr. Malama's Soil Exploration of the Kendall Site and New Boreholes B1 and B2. Arroyo Grande, CA: Creek Lands Conservation.

D. W. Alley & Associates. (2008). *Santa Rosa Creek fishery summary, habitat conditions, watershed management guidelines, and enhancement goals*.

DWR. (2021). *California's Groundwater Update 2020. Bulletin 118 Draft.* Retrieved from https://water.ca.gov/Californias-Groundwater

Freeze, A. Cherry, J. (1979) *Groundwater.* Retrieved from http://hydrogeologistswithoutborders.org/wordpress/1979-english/

Ishida, S. (2010). S*ustainable Use of Groundwater with Underground Dams*. Retrieved from https://www.jstage.jst.go.jp/article/jarq/45/1/45_1_51/_article

Japan Green Resources Agency (JGRC) (2006) *Policy for Creating Plans for Subsurface Dams, eds. Hasegawa T. et al., Guide to Water Resource Development Using Subsurface Dams*.

Malama, B., Solum, J., & Nicholson, B. (2019). *Results of Direct-Push Exploratory Borehole Drilling at the Kendall Site for the Santa Rosa Creek Flow Enhancement Pilot Project.* California Polytechnic State University, San Luis Obispo, California, San Luis Obispo.

Moriasi, N. D. (2015). *Hydrologic and Water Quality Models: performance Measures and Evaluation Criteria.*

Muleta, M. (2021). *In-Progress Model of the Santa Rosa Creek Watershed.* California Polytechnic State University San Luis Obispo, Civil and Environmental Engineering.

Murray, A. (2020). *Modeling Artificial Groundwater Recharge in the Santa Rosa Creek Watershed.*

National Marine Fisheries Service. (2006). *Endangered and threatened species; revision of species of concern list, candidate species definition, and candidate species list*. Retrieved from https://www.federalregister.gov/documents/2006/10/17/E6-17249/endangered-and-threatened-species-revision-of-species-of-concern-list-candidate-species-definition

Nelson, J., E. Baglivio, and T. Kahles. (2009). *Santa Rosa Creek Steelhead Habitat and Population Survey, 2005*.

PG&E. (2013). *PG&E Diablo Canyon Power Plant (DCPP): San Simeon, CA Central Coast*. Retrieved from OpenTopography: https://portal.opentopography.org/raster?opentopoID=OTSDEM.032013.26910.2

Stillwater Sciences, Central Coast Salmon Enhancement, and Greenspace – The Cambria Land Trust. (2012). *Santa Rosa Creek Watershed Management Plan.*

Stillwater Sciences. (2021). *Basis of Design Report for the Santa Rosa Creek Stream Flow Enhancement Pilot Project (65% Design Level)*.

Todd, K. D., & Mays, W. L. (2005). *Groundwater Hydrology, 3rd Edition*. United States of America: John Wiley & Sons, Inc.

USDA. (2021). *Saturated hydraulic conductivity in relation to soil texture.* Retrieved from https://www.nrcs.usda.gov/wps/portal/nrcs/detail/soils/survey/office/ssr10/tr/?cid=nrcs144p2_074846

USGS. (2020). *Groundwater Information by Topic*. Retrieved from Water Science School: https://www.usgs.gov/special-topic/water-science-school/science/groundwater-information-topic?qt-science_center_objects=0#qt-science_center_objects

Watershed Progressive. (2021). *In Progress 65% Basis of Design Report.*

Yates, E. B., & Van Konyenburg, K. M. (1998). *Hydrogeology, Water Quality, Water Budgets, and Simulated Responses to Hydrologic Changes in Santa Rosa and San Simeon Creek Ground-Water Basins, San Luis Obispo County, California.* Sacramento: USGS.

Yeh, H. (2018). *Analyzing the Effect of Soil Hydraulic Conductivity Anisotropy on Slope Stability Using a Coupled Hydromechanical Framework.*